NACA

# RESEARCH MEMORANDUM



## EFFECTS OF INLET AIR DISTORTION ON STEADY-STATE PERFORMANCE OF AN AXIAL-FLOW TURBOJET ENGINE

By Robert E. Russey and Ferris L. Seashore

Lewis Flight Propulsion Laboratory
Cleveland, Ohio



NATIONAL ADVISORY COMMITTEE
FOR AERONAUTICS
WASHINGTON

40

# EFFECTS OF INLET AIR DISTORTION ON STEADY-STATE PERFORMANCE OF AN AXIAL-FLOW TURBOJET ENGINE

By Robert E. Russey and Ferris L. Seashore



## ABSTRACT

Conditions simulated flight at Mach 0.8 at a 35,000-ft altitude. Data were obtained for distortion magnitudes of 15, 22, and 27 percent, which were contained within a 70° sector of the inlet annulus. The circumferential extent of a 15-percent flow distortion was varied from 20° to 168°. The severity of the turbine temperature gradients increased and the compressor performance dropped off as the magnitude and circumferential extent of the flow distortions were increased, while the performance of the combustor and turbine remained essentially unchanged. The reduction in compressor performance resulted in a net-thrust loss of 3.5 percent for the most severe distortion configuration investigated.

## INDEX HEADINGS

Engines, Turbojet 3.1.3

Engines, Control - Turbojet 3.2.2

Compressors - Axial Flow 3.6.1.1

NACA RM E57L31

NATIONAL ADVISORY COMMITTEE FOR AERONAUTICS

RESEARCH MEMORANDUM

# EFFECTS OF INLET AIR DISTORTION ON STEADY-STATE PERFORMANCE OF AN AXIAL-FLOW TURBOJET ENGINE

By Robert E. Russey and Ferris L. Seashore



## SUMMARY

An investigation was conducted in an altitude facility at the NACA Lewis laboratory to determine the effects of magnitude and circumferential extent of inlet total-pressure distortions on the over-all and component performance of a current turbojet engine. The circumferential extent and magnitude of the flow distortions could be progressively varied between two physical limits. It was also possible to hold the magnitude of the flow distortion constant over a range of corrected engine speed. Data were obtained at an engine-inlet Reynolds number index of 0.44 (corresponding to an altitude of 35,000 ft at a flight Mach number of 0.8).

Although the turbine temperature profiles were affected slightly by the distortions, the performance of the combustor and turbine remained essentially unchanged. Compressor and, consequently, over-all engine performance were affected, however, as either the circumferential extent or magnitude of distortion was increased, with the greatest losses occurring at reduced engine speed. A loss of about 2 percent in compressor efficiency and corrected airflow occurred at approximately rated speed with the most severe distortion configuration investigated. This loss in compressor performance resulted in a 3.5-percent decrease in maximum net thrust and a 1-percent increase in specific fuel consumption.

## INTRODUCTION

Inlet airflow distortion, a nonuniform distribution of airflow and total pressure at the engine inlet, can occur as a result of operation of air inlets at off-design mass-flow ratios, flow separation within the inlet air ducting, or operation of the aircraft at high angles of attack or yaw. Previous investigations conducted at this laboratory (refs. 1 to 4) have shown that operation of an engine with nonuniform inlet pressure distributions present can result in severe performance penalties, such as reduced thrust and increased specific fuel consumption. These

losses in over-all engine performance usually are the result of off-design operation of the compressor, which is the component most susceptible to inlet distortions. Off-design operation of the compressor may also be responsible for the occurrence of surge or rotating stall, which can cause excessive compressor blade vibrations or severe turbine-inlet temperature profiles and result in structural failure of the compressor or turbine (ref. 5).

The effects of magnitude and extent of circumferential inlet pressure distortions on the performance of a high-pressure-ratio, axial-flow turbojet engine were investigated in an altitude test facility as a part of a general program conducted at the NACA Lewis laboratory. The effect on steady-state performance is reported herein, and the effect on the surge characteristics and persistence of distortion in the compressor is presented in reference 6. Previous investigations of the inlet distortion problem were conducted using fixed inlet screens to obtain a low-pressure area at the compressor inlet; and, since the pressure loss through a screen is a function of airflow (corrected engine speed), the amplitude (magnitude) of the distortion could not be maintained constant over a range of engine speeds.



For that portion of the investigation reported herein, an inlet distortion rig was used which (1) provided constant magnitude of total-pressure distortion over a range of engine speeds, (2) permitted variation of circumferential extent of distortion, and (3) permitted rotation of circumferential extent of distortion past transient instrumentation in order to obtain a detailed picture of the persistence of the distortion throughout the engine.

The effects of distortion magnitude are defined for a $70^{\circ}$ sector of the inlet annulus, and the effects of circumferential extent of distortion are defined for a magnitude $\Delta P/P$ of 15 percent. Data were obtained at an engine-inlet Reynolds number index of 0.44 (corresponding to an altitude of 35,000 ft at a flight Mach number of 0.8) and are presented primarily for rated exhaust-nozzle area over a range of corrected engine speeds.

## APPARATUS

### Engine and Installation

The high-pressure-ratio turbojet engine used has a 15-stage axial-flow compressor, a cannular-type combustor with eight tubular liners, and a two-stage turbine. The compressor has progressively variable inlet guide vanes and a two-position acceleration bleed valve located at the seventh stage. Data presented herein were obtained with the high-speed compressor configuration (inlet guide vanes open and acceleration bleed valve closed).

[redacted]

The engine was equipped with a $62\frac{3}{4}$-inch-long tailpipe and a variable-area exhaust nozzle (clamshell type). At an engine speed of 7800 rpm with rated exhaust-nozzle area, the turbine-outlet temperature was 1220° F (1680° R). The engine was installed in an altitude test facility (fig. 1), where inlet pressure and temperature and ambient exhaust pressure could be regulated to simulate altitude flight conditions.

### Inlet Distortion Rig

A photograph of the inlet distortion rig installed on the engine is presented in figure 1, and a cutaway sketch of the distortion rig is presented in figure 2. The magnitude of the inlet total-pressure distortions obtainable with this rig was independent of corrected engine speed (corrected airflow). Distortions are usually simulated by obtaining a pressure loss through a screen that is located upstream of the compressor inlet. The pressure loss obtained is a function of engine airflow and therefore does not remain constant for a range of engine speed. The subject distortion rig, however, incorporated an air bleed system downstream of the screen, which made it possible to maintain constant pressure loss through that portion of the inlet screen that was located upstream of the distorted sector.

The circumferential extent of the distorted section could be set to any desired angular sector, from a minimum of 8° to a maximum of 168°, by means of the movable splitter vane. Maximum distortion magnitude was limited to 15 and 27 percent with sector angles of 168° and 70°, respectively, because of a limit in the capacity of the air bleed system. The sector containing the distortion could also be rotated about the face of the compressor.

## INSTRUMENTATION

Steady-state transient instrumentation used during the portion of the investigation reported herein was installed at various stations throughout the engine, as shown in figure 3. Engine fuel flow was measured with calibrated rotameters, and engine speed was measured with a remote-reading electronic tachometer. Engine thrust was calculated from pumping characteristics.

## PROCEDURE

Data were obtained at a Reynolds number index of 0.44 (which corresponds to an altitude of 35,000 ft at a flight Mach number of 0.8) over a range of corrected engine speed. Free-stream inlet total pressure

[redacted]

$P_{1,U}$ corresponding to complete ram recovery at the above flight condition was set in the undistorted sector at the engine inlet (downstream of the screen), and the pressure $P_{1,D}$ required to give the desired distortion magnitude $(P_{1,U} - P_{1,D})/P_{1,U}$ was set in the distorted sector. The pressure $P_{1,D}$ was set by regulating the flow of bleed-off air from the distorted sector.

Data for comparison with the uniform inlet flow performance were obtained with the distortion configurations shown in the following table:

| Distortion, $\frac{P_{1,U} - P_{1,D}}{P_{1,U}}$, percent | Sector angle, deg | | | |
|---|---|---|---|---|
| | 20 | 40 | 70 | 168 |
| 15 | x | x | x | x |
| 22 | | | x | |
| 27 | | | x | |

The fixed exhaust-nozzle area actually varied during the investigation because of changing air loads on the clamshell nozzle. The variation in effective exhaust-nozzle area is shown in figure 4 as a function of corrected engine speed. In addition, the effective exhaust-nozzle area deviated from that indicated in figure 4 by as much as ±1.5 percent. This deviation was essentially constant for a given distortion configuration and was considered small enough to limit the effect on component performance to experimental error. Therefore, component performance is compared on the basis of fixed exhaust-nozzle area. Over-all engine performance, however, could not be compared in the same manner. Consequently, engine pumping characteristics for each configuration were calculated from the performance of the engine components at equal values of engine total-temperature ratio.

For that portion of the investigation reported herein, total- and static-pressure profiles at the compressor-inlet guide vanes were obtained by slowly rotating the distorted sector past fixed instrumentation and recording the transient variation in these pressures. With the above exception, all data presented herein were obtained with the distortion configurations centered on an inlet circumferential location of 45° (measured clockwise from top of engine, looking downstream).

An area-weighted average value of compressor-inlet total pressure $P_{1,av}$ was used in the calculation of the engine performance parameters

presented herein. The symbols used in this report are defined in appendix A, and the methods of calculation are presented in appendix B.

## RESULTS AND DISCUSSION

### Pressure and Temperature Profiles

4634

Typical circumferential, midspan pressure and temperature profiles which existed at the inlet-guide-vane, compressor-outlet, and turbine-outlet stations are presented for the various distortion configurations investigated.

Total-pressure profiles at the inlet-guide-vane station are presented in figure 5 for some of the distortion configurations investigated. The variation in total pressure for inlet pressure distortions $\Delta P/P$ of 15 and 22 percent with a sector angle of $70^{\circ}$ is shown in figure 5(a), while figure 5(b) shows the pressure variation for sector angles of $70^{\circ}$ and $168^{\circ}$ with a $\Delta P/P$ of 15 percent. The ratio of local pressure with distortion to average pressure with uniform flow $P_{1,U}$ is used as the ordinate in order to form a basis for comparison of the different distortion configurations. A portion of the $168^{\circ}$ sector profile is shown by dashes because the limit of rotation of the apparatus was reached before the profile could be fully defined. Rotation of the distorted sector past the fixed instrumentation resulted in a small change in inlet conditions because of a change in position of the seals which separated the high- and low-pressure sectors. Consequently, the pressure on the left side of the distortion was usually slightly higher than that on the right side. The value of $\Delta P/P$ actually obtained also varied somewhat from the nominal value of $\Delta P/P$ because of this rotation. The difficulty in maintaining inlet conditions was not encountered when the distorted sector was stationary.

Static-pressure profiles, which were measured at a station 4 inches upstream of the inlet guide vanes, are presented for inlet pressure distortions of 15 and 22 percent with a sector angle of $70^{\circ}$ (fig. 6(a)) and for sector angles of $70^{\circ}$ and $168^{\circ}$ for a $\Delta P/P$ of 15 percent (fig. 6(b)). Inlet velocity distortions, based on steady-state inlet total and static pressures, increased as corrected engine speed was reduced. An increase in velocity distortion of about 5 percent occurred as corrected engine speed was reduced from 7800 to 6600 rpm.

The compressor-outlet total-pressure profiles of figure 7 indicate that the circumferential pressure gradient at this station was only slightly affected by the most severe distortion configurations investigated. A 1-percent variation in the circumferential pressure distribution occurred with the $168^{\circ}$ sector configuration, while the pressure gradients obtained with the other distortion configurations were less

than 1 percent. The ratio of the local to the average value of pressure with distortion is used in the numerator of the ordinate in order to establish a common basis for comparison, and the local-to-average ratio for uniform flow is used in the denominator in order to eliminate slight deviations in the undistorted profile.

The total-temperature profiles presented in figure 8(a) indicate that a temperature gradient existed at the compressor outlet. The temperature profile became more severe as both magnitude and circumferential extent of distortion increased. The temperature gradient indicates that a greater amount of work is done by the compressor within the distorted sector.



The apparent peak in compressor-outlet total temperature is located at 165°, while the distortion was centered at a compressor-inlet location of 45°. This indicates a displacement of the distortions in the direction of compressor rotation as they passed through the compressor. This angular displacement corresponds to an approximate mean flow path which was calculated for the compressor.

Typical turbine-outlet total-temperature profiles are presented in figure 8(b). The temperature gradients at this station appear similar to those which existed at the compressor outlet, but are more severe.

## Component Performance

The effects of both magnitude of distortion $\Delta P/P$ and circumferential extent of distortion (sector angle) on component performance are compared separately with the uniform inlet flow performance. It should be noted that the 70° sector angle, 15-percent distortion condition is common to both comparisons.

Compressor. - Corrected inlet airflow $w_{a,1}\sqrt{\theta_1}/\delta_{1,av}$, which was calculated by assuming the existence of choked flow at the turbine inlet, is presented in figures 9(a) and (b) as a function of corrected engine speed $N/\sqrt{\theta_1}$. The effect of the magnitude of distortion $\Delta P/P$ is shown in figure 9(a). As $\Delta P/P$ increased, the reduction in corrected airflow became progressively larger so that, for the maximum $\Delta P/P$ investigated (27 percent), corrected airflow was reduced 2 percent at a corrected engine speed of 7800 rpm (fig. 9(a)). Operation at 6600 rpm with the same distortion magnitude resulted in an 8.6-percent decrease in corrected airflow. A similar reduction in corrected airflow occurred as the circumferential extent of distortion (sector angle) was increased (fig. 9(b)). For the largest sector angle investigated (168°), an airflow reduction of 1.7 percent occurred at a corrected engine speed of 7800 rpm, and a reduction of 6.2 percent occurred at 6600 rpm.

Compressor over-all pressure ratio $P_2/P_{1,av}$ is presented in figures 9(c) and (d) as a function of corrected engine speed. Increasing distortion magnitude caused a decrease in over-all pressure ratio (fig. 9(c)). Operation with the 27-percent distortion at a corrected engine speed of 7800 rpm resulted in a 3.2-percent drop in pressure ratio. A pressure ratio loss of 10 percent occurred at 6600 rpm with the same distortion magnitude. Increasing the circumferential extent of distortion also resulted in a reduction of over-all pressure ratio (fig. 9(d)). Operation with the 168° sector angle resulted in a pressure ratio drop of about 1 percent at a corrected engine speed of 7800 rpm, while a loss of 5.2 percent occurred with the same configuration at 6600 rpm.



Compressor efficiency (based on $P_{1,av}$) is shown as a function of corrected engine speed in figure 9(e). Increasing distortion magnitude caused compressor efficiency to drop. A loss of about 2 percent in efficiency occurred at 7800 rpm with the 27-percent distortion, and an efficiency drop of 5.5 percent occurred at 6600 rpm. A similar reduction in efficiency occurred as the circumferential extent of distortion was increased, with maximum losses of 2.5 and 4.8 percent occurring at corrected speeds of 7800 and 6600 rpm, respectively.

The losses in compressor performance increased as corrected engine speed was reduced because the loading of the inlet stages of the compressor was increased by flow distortion. At low corrected speeds, where the loading of the inlet stages is normally high, the performance of these stages is affected by an increase in loading due to flow distortion. At high corrected speeds, however, the loading of the inlet stages is relatively low and therefore is less sensitive to increases in loading. Although the loading of the rear stages of the compressor is normally high at high corrected speed, the increase in loading due to flow distortion is small because the flow distortions diminish considerably in magnitude in passing through the compressor.

Combustor. - Combustion efficiency is presented in figure 10 as a function of a combustion parameter $w_{a,2}T_6$. Although the parameter PT/V is commonly used to generalize combustion efficiency, PT/V is approximately proportional to the parameter $w_{a,2}T_6$, which is easier to obtain (ref. 7). The apparent slight shift in combustion efficiency could be due to a nonuniformity in the circumferential fuel-air ratio distribution. However, if the limits of accuracy of these data are considered, it is believed that the slight shift in efficiency is not meaningful.

Turbine. - Turbine efficiency is presented in figure 11 as a function of corrected engine speed. Within the accuracy of these data, turbine efficiency was insensitive to changes in magnitude and circumferential extent of distortion. For all the configurations investigated, turbine efficiency was about 91 percent at a corrected engine speed of

[redacted]

7800 rpm. Decreasing engine speed to 6600 rpm resulted in a 1-percent drop in efficiency.

### Engine Pumping Characteristics

As previously mentioned in the section PROCEDURE, engine pumping characteristics for each configuration were calculated from the component performance at equal values of engine total-temperature ratio. The values of engine temperature ratio used in the calculation are presented in figure 12 as a function of corrected engine speed. This curve was obtained with uniform inlet flow.

The engine pumping characteristics are presented in figure 13. A reduction in engine pressure ratio occurred as either circumferential extent or magnitude of distortion was increased at constant engine temperature ratio. The drop in pressure ratio that occurred with a given distortion configuration increased as engine temperature ratio decreased. The occurrence of greater losses in pressure ratio at the lower engine temperature ratios reflects the correspondingly larger compressor performance losses at reduced engine speeds.

### Net Thrust and Net-Thrust Specific Fuel Consumption

Maximum net thrust, which was calculated from engine pumping characteristics, was obtained at a corrected engine speed of 7800 rpm with rated exhaust-nozzle area. That portion of the net-thrust loss due to the reduction of average inlet total pressure by flow distortion was excluded by using maximum inlet total pressure in the calculation of maximum net thrust. Consequently, the loss in net thrust and the increase in net-thrust specific fuel consumption reflect only the changes in compressor performance that were caused by the inlet flow distortions.

The effect of distortion magnitude on maximum net thrust and net-thrust specific fuel consumption is presented in figure 14(a). A 3.5-percent loss in maximum net thrust and a 1-percent increase in net-thrust specific fuel consumption occurred with a distortion magnitude of 27 percent. The effect of circumferential extent of distortion on maximum net thrust and net-thrust specific fuel consumption is shown in figure 14(b). Operation with the 168° sector angle resulted in a 2.5-percent decrease in maximum net thrust and an increase in net-thrust specific fuel consumption of approximately 0.5 percent.

## SUMMARY OF RESULTS

An investigation was conducted to determine the effects of magnitude and circumferential extent of inlet total-pressure distortion on

the over-all and component performance of a current turbojet engine. The circumferential extent and magnitude of the distortion configurations could be held constant over a range of corrected engine speeds. Data were obtained at a Reynolds number index of 0.44 (corresponding to an altitude of 35,000 ft at a flight Mach number of 0.8).

Although these distortions persisted through the compressor, the magnitude of the total-pressure gradient at the compressor outlet was greatly diminished. The severity of the total-temperature gradient that existed at the compressor outlet increased slightly at the turbine outlet, which indicates a small effect on the fuel-air ratio distribution. The severity of the temperature gradients increased as the magnitude or circumferential extent of the flow distortion increased. The location of the peak in the compressor-outlet total-temperature gradient indicated that a rotational translation of the flow distortions occurred as they passed through the compressor. This translation corresponded to an approximate mean flow path which was calculated for the compressor.

The performance of the combustor and turbine was essentially unchanged by the flow distortions investigated, but the compressor performance was reduced as the distortions were increased in severity. The reduction in compressor performance was reflected in a decrease in over-all engine performance. The effect of inlet flow distortion on performance was greatest for operation at reduced engine speed. At rated corrected engine speed, a 2-percent decrease in compressor efficiency and corrected airflow occurred for operation with the most severe distortion configuration. A maximum net-thrust loss of 3.5 percent and a 1-percent increase in net-thrust specific fuel consumption resulted from operation with the same configuration.

Lewis Flight Propulsion Laboratory
National Advisory Committee for Aeronautics
Cleveland, Ohio, January 3, 1958



[redacted]

## APPENDIX A

## SYMBOLS

| | |
|---|---|
| $A$ | area, sq ft |
| $F_n$ | net thrust, lb |
| $g$ | acceleration due to gravity, $ft/sec^2$ |
| $h$ | enthalpy, Btu/lb |
| $N$ | engine speed, rpm |
| $P$ | total pressure, lb/sq ft |
| $p$ | static pressure, lb/sq ft |
| $T$ | total temperature, $^{\circ}R$ |
| $V$ | velocity, ft/sec |
| $w_a$ | airflow, lb/sec |
| $w_f$ | fuel flow, lb/sec |
| $w_g$ | gas flow, lb/sec |
| $\beta$ | function of $\gamma$, $\frac{1.4}{\gamma}\frac{\left(\frac{\gamma+1}{2}\right)^{\frac{\gamma}{\gamma-1}}}{\left(\frac{1.4+1}{2}\right)^{\frac{1.4}{1.4-1}}}$ |
| $\gamma$ | ratio of specific heats |
| $\delta$ | ratio of absolute total pressure to absolute static pressure of ICAO standard atmosphere at sea level |
| $\eta$ | efficiency |
| $\theta$ | ratio of absolute total temperature to absolute static temperature of ICAO standard atmosphere at sea level |
| $\theta_{cr}$ | squared ratio of critical velocity to critical velocity at ICAO standard sea-level conditions, $(V_{cr}/1018)^2$ |

4634

[redacted]

Subscripts:

| | |
|---|---|
| av | average |
| B | combustor |
| C | compressor |
| cr | critical |
| D | distorted |
| eff | effective |
| j | vena contracta at exhaust-nozzle outlet |
| T | turbine |
| U | undistorted |
| 0 | free stream |
| 1 | compressor inlet |
| 2 | compressor outlet |
| 3 | turbine inlet |
| 4 | turbine outlet |
| 6 | exhaust-nozzle inlet |
| 10 | exhaust-nozzle outlet |

# APPENDIX B

## METHODS OF CALCULATION

### Averaging of Total Pressures and Temperatures

The average compressor-inlet total pressure was determined by area-averaging the total pressures which were measured in the distorted and undistorted sectors of the compressor inlet according to the following equation:

$$P_{1,av} = \frac{P_{1,U} A_{1,U} + P_{1,D} A_{1,D}}{A_{1,U} + A_{1,D}}$$

All other pressures and temperatures were determined by arithmethic averages.

### Compressor and Turbine Efficiencies

The efficiencies were evaluated using the conventional adiabatic equations. Average values of pressure and temperature, as previously defined, were used in evaluating efficiency.

### Combustion Efficiency

Engine combustion efficiency is defined as the ratio of the ideal engine fuel flow to the actual fuel flow. The ideal flow is defined as the fuel flow required to satisfy a heat balance across the engine by using measured temperatures, airflow, and an ideal combustion process. Fuel flows associated with an ideal combustion process were obtained from reference 8.

### Turbine-Inlet Temperature

Turbine-inlet temperature was calculated by means of a heat balance across the combustor by using the measured combustor-inlet temperature and the ideal fuel flow as obtained from reference 8.

### Engine Total-Pressure Ratio

The engine total-pressure ratio for each configuration was calculated for a range of corrected engine speeds by using the corrected



[redacted]

inlet airflow and component performance as presented in figures 9 to 11. The engine total-temperature ratio at a given corrected engine speed for each distortion configuration was assumed to equal the temperature ratio that was obtained with uniform inlet flow (fig. 12).

The assumption of an altitude and a flight Mach number (35,000 ft and 0.8, respectively) specified values of $P_1$, $T_1$, $p_0$, $\delta_1$, and $\sqrt{\theta_1}$. Corrected inlet airflow for a given configuration was then determined from figures 9(a) and (b) and the desired value of corrected engine speed. Compressor-inlet airflow, based on the assumption of 100-percent ram pressure recovery, was then calculated according to the following equation:



$$w_{a,1} = \frac{w_{a,1}\sqrt{\theta_1}}{\delta_{1,av}} \frac{1}{\sqrt{\theta_1}} \frac{P_1}{2116}$$

Airflows at other stations within the engine were calculated according to the following equations:

$$w_{a,2} = w_{a,6} = 0.978\ w_{a,1}$$

$$w_{a,3} = 0.986\ w_{a,2}$$

The constants in the above equation account for the compressor seal leakage and turbine cooling airflows.

The turbine-inlet total temperature was calculated as previously outlined, using the combustor-inlet total temperature obtained from figure 15. Turbine-inlet total pressure was calculated by assuming choked flow at the turbine inlet:

$$P_3 = w_{g,3}\sqrt{\theta_{cr,3}}\ \beta_3\ 48.20$$

Turbine-outlet total pressure was then calculated from the turbine efficiency and turbine work.

## Net Thrust

The calculation of net thrust was based on engine pumping characteristics. The thrust equation used is:

$$F_n = \left[\frac{w_{g,6}}{g} V_j + A_j(p_j - p_0)\right] - \frac{w_{a,1}V_0}{g}$$

[redacted]

The parameter enclosed in brackets is most easily solved by means of the effective velocity parameter of reference 9 together with $w_{g,6}$, $T_6$, $\gamma_6$, and $p_0/h_6$.

## Specific Fuel Consumption

The net-thrust specific fuel consumption sfc was calculated from

$$sfc = \frac{w_f}{F_n}$$

4634

## REFERENCES

1. Harry, David P., III, and Lubick, Robert J.: Inlet-Air Distortion Effects on Stall, Surge, and Acceleration Margin of a Turbojet Engine Equipped with Variable Compressor Inlet Guide Vanes. NACA RM E54K26, 1955.

2. Huntley, S. C., Sivo, Joseph N., and Walker, Curtis L.: Effect of Circumferential Total-Pressure Gradients Typical of Single-Inlet Duct Installations on Performance of an Axial-Flow Turbojet Engine. NACA RM E54K26a, 1955.

3. Smith, Ivan D., Braithwaite, W. M., and Calvert, Howard F.: Effect of Inlet-Air-Flow Distortions on Steady-State Performance of J65-B-3 Turbojet Engine. NACA RM E55I09, 1956.

4. Fenn, David B., and Sivo, Joseph N.: Effect of Inlet Flow Distortions on Compressor Stall and Acceleration Characteristics of a J65-B-3 Turbojet Engine. NACA RM E55F20, 1955.

5. Walker, Curtis L., Sivo, Joseph N., and Jansen, Emmert T.: Effect of Unequal Air-Flow Distribution from Twin Inlet Ducts on Performance of an Axial-Flow Turbojet Engine. NACA RM E54E13, 1954.

6. Ciepluch, Carl C.: Effect of Inlet Air Distortion on the Steady-State and Surge Characteristics of an Axial-Flow Turbojet Compressor. NACA RM E57L12, 1958.

7. McAulay, John E., and Kaufman, Harold R.: Altitude Wind Tunnel Investigation of the Prototype J-40-WE-8 Turbojet Engine Without Afterburner. NACA RM E52K10, 1953.

[redacted]

8. Huntley, S. C.: Ideal Temperature Rise Due to Constant-Pressure Combustion of a JP-4 Fuel. NACA RM E55G27a, 1955.

9. Turner, L. Richard, Addie, Albert N., and Zimmerman, Richard H.: Charts for the Analysis of One-Dimensional Steady Compressible Flow. NACA TN 1419, 1948.



[redacted]

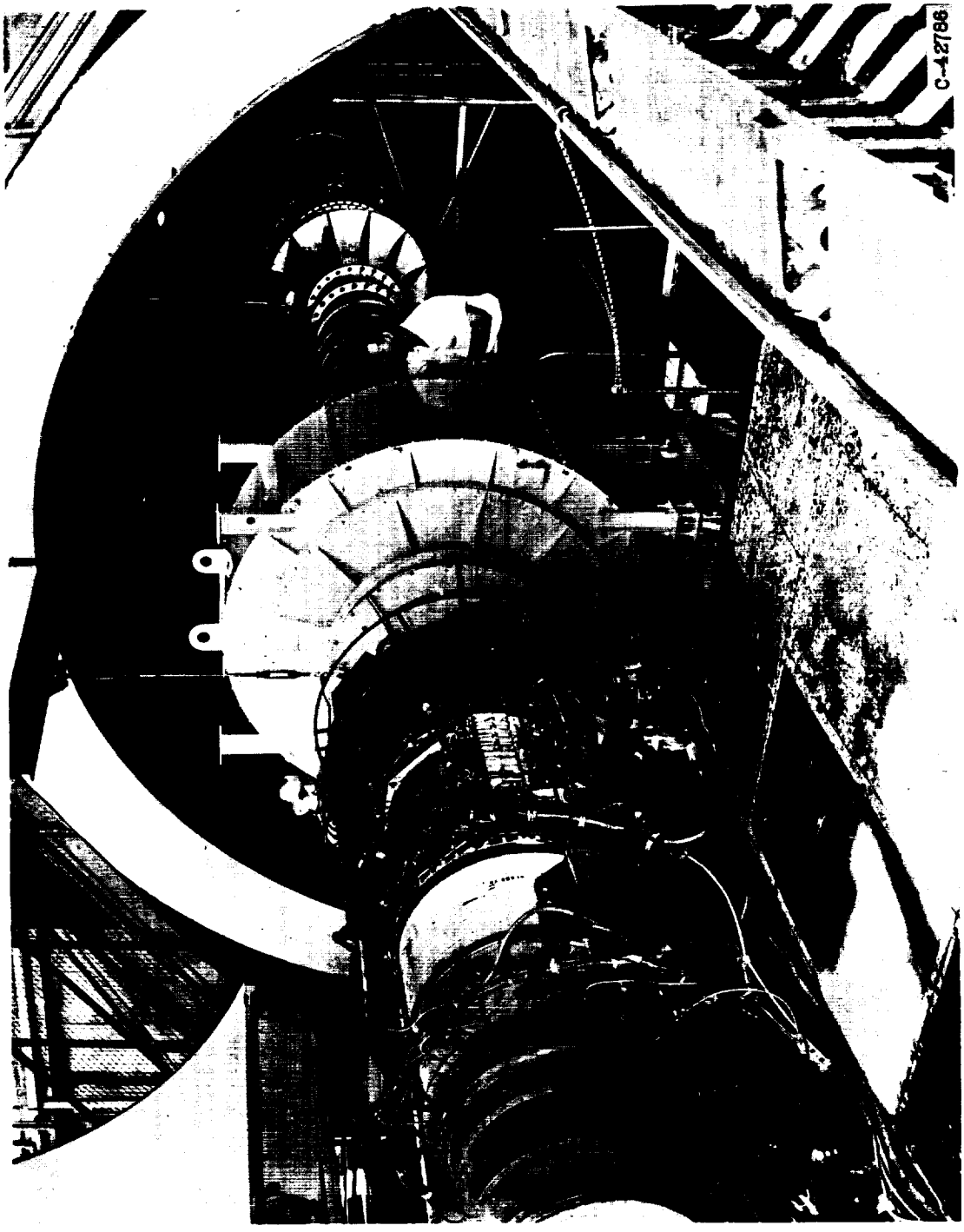


Figure 1. - Engine installed in altitude test facility.

4634

CI-3

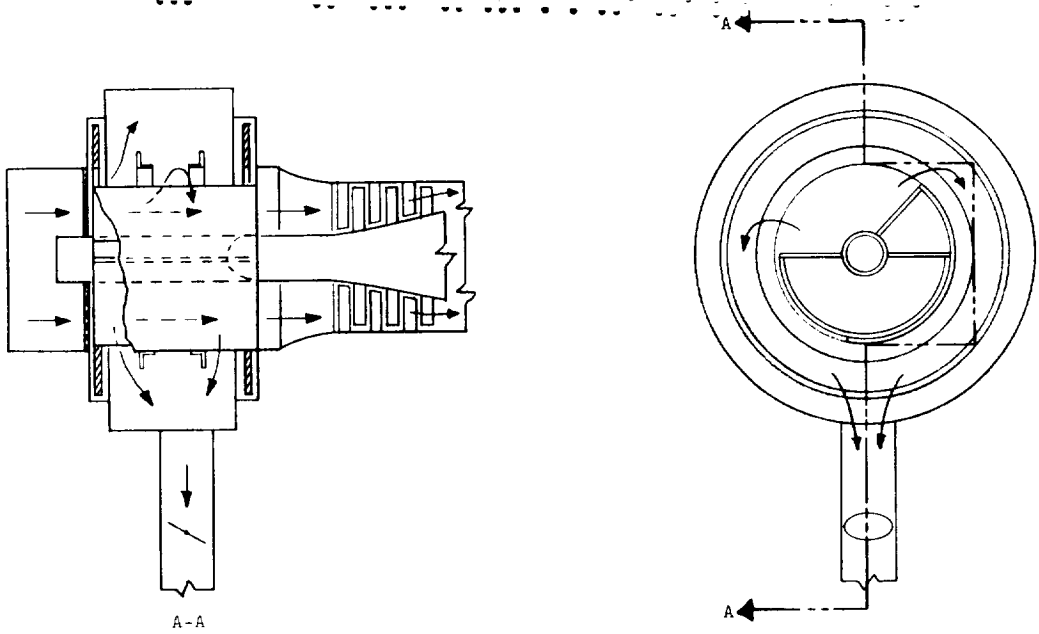


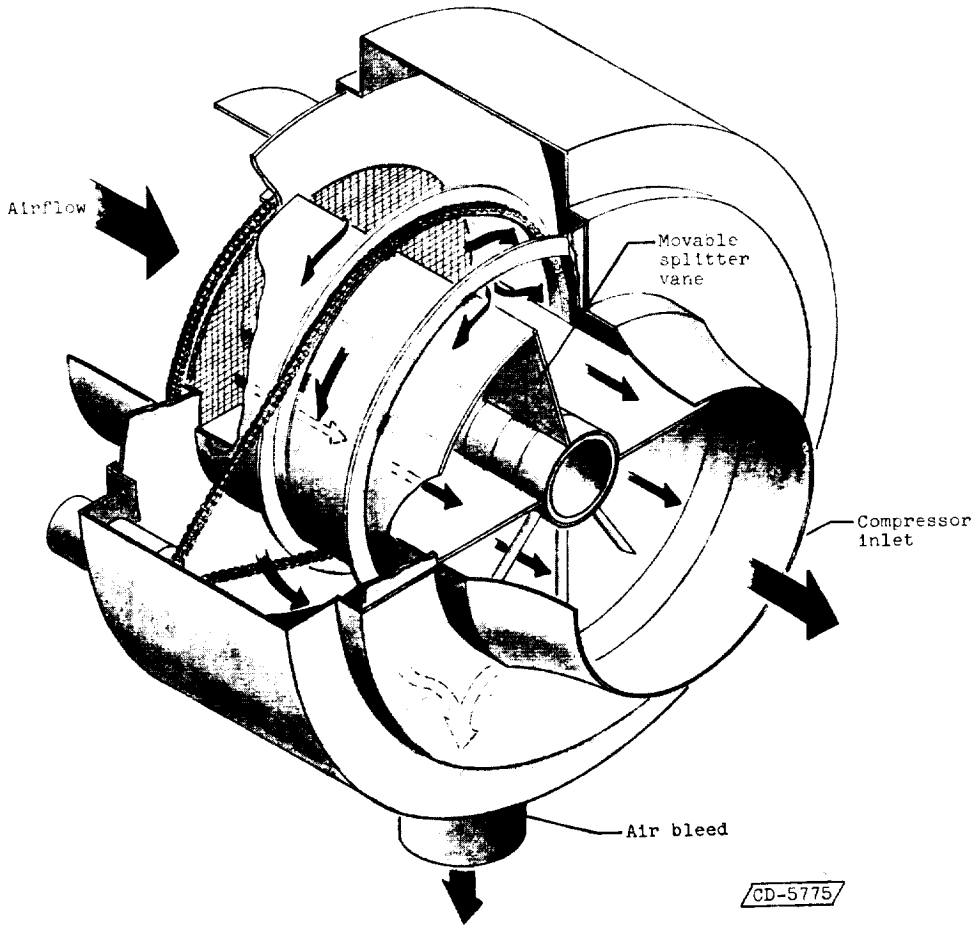


Figure 2. - Inlet distortion rig.

[redacted]

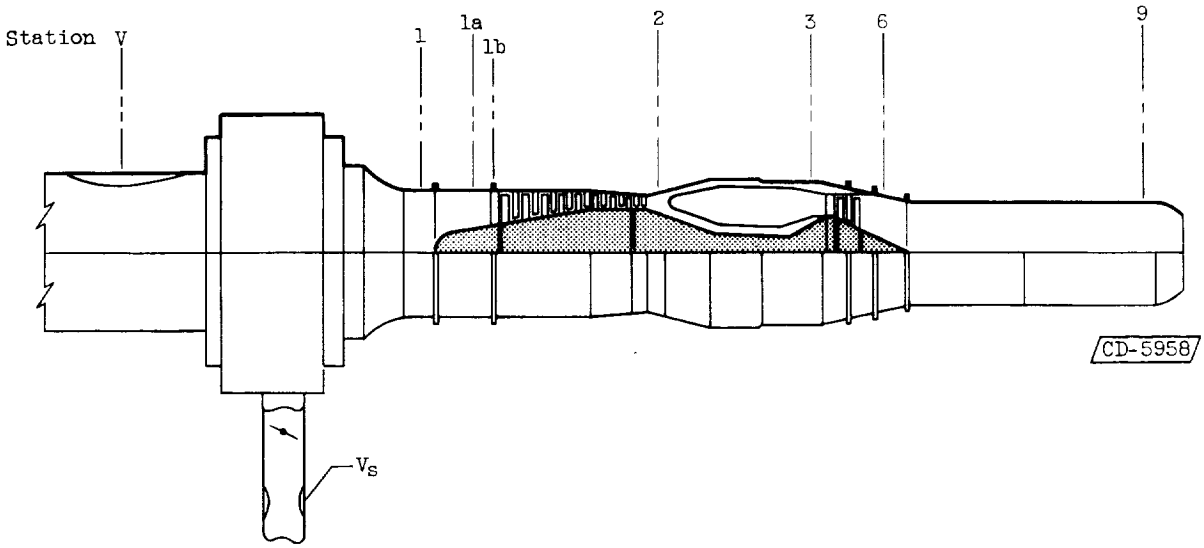


STEADY-STATE INSTRUMENTATION

| Station | Location | Total-pressure probes | Static-pressure tubes | Wall static-pressure orifices | Thermocouples |
|---|---|---|---|---|---|
| V | Venturi | 18 | 5 | 2 | 4 |
| $V_S$ | Small venturi (bleed) | 6 | 3 | 2 | 2 |
| 1 | Compressor inlet | 46 | 14 | 8 | 12 |
| 2 | Compressor outlet | 20 | 0 | 3 | 23 |
| 3 | Turbine inlet | 12 | - | - | 28 |
| 6 | Turbine outlet | 18 | - | - | 30 |
| 9 | Exhaust-nozzle inlet | 16 | - | - | 26 |

TRANSIENT INSTRUMENTATION

| Station | Location | Type of probe | |
|---|---|---|---|
| 1a | 4 In. upstream of inlet guide vanes | 1 Nondirectional static pressure | Variable-reluctance, diaphragm-type pressure tranducer |
| 1b | Plane of inlet guide vanes | 1 Total pressure | |

Figure 3. - Transient and steady-state instrumentation of turbojet engine.

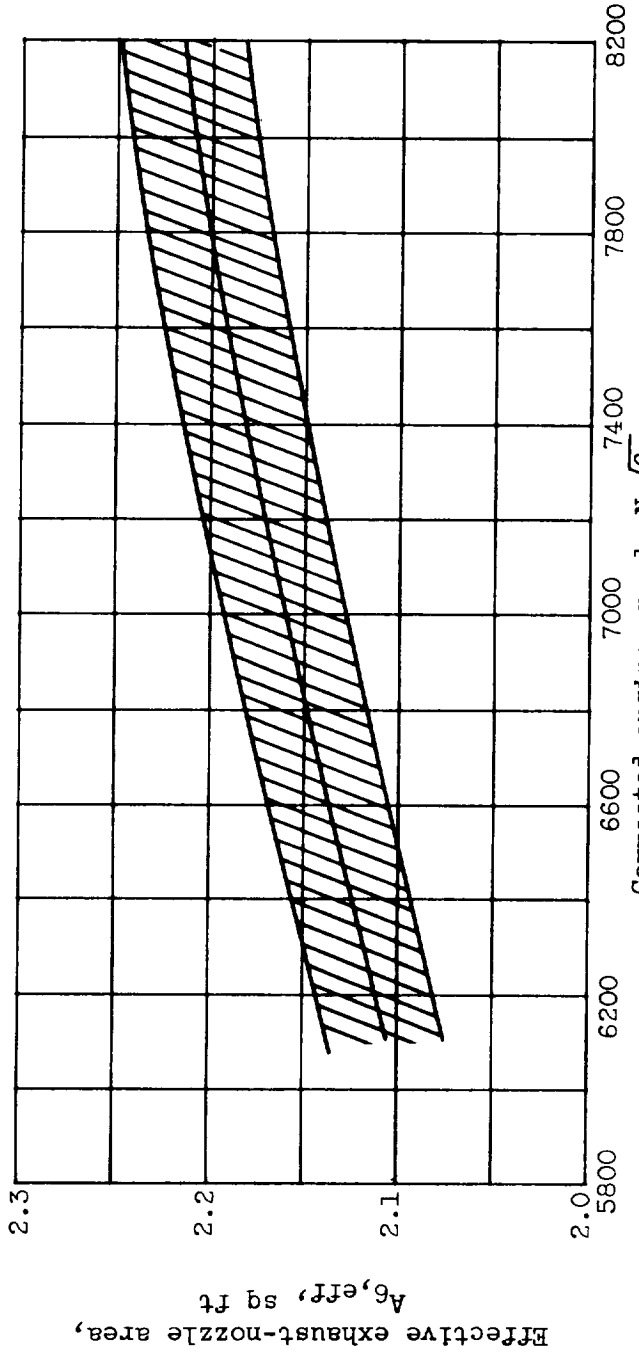


Figure 4. - Variation of effective exhaust-nozzle area for all configurations.

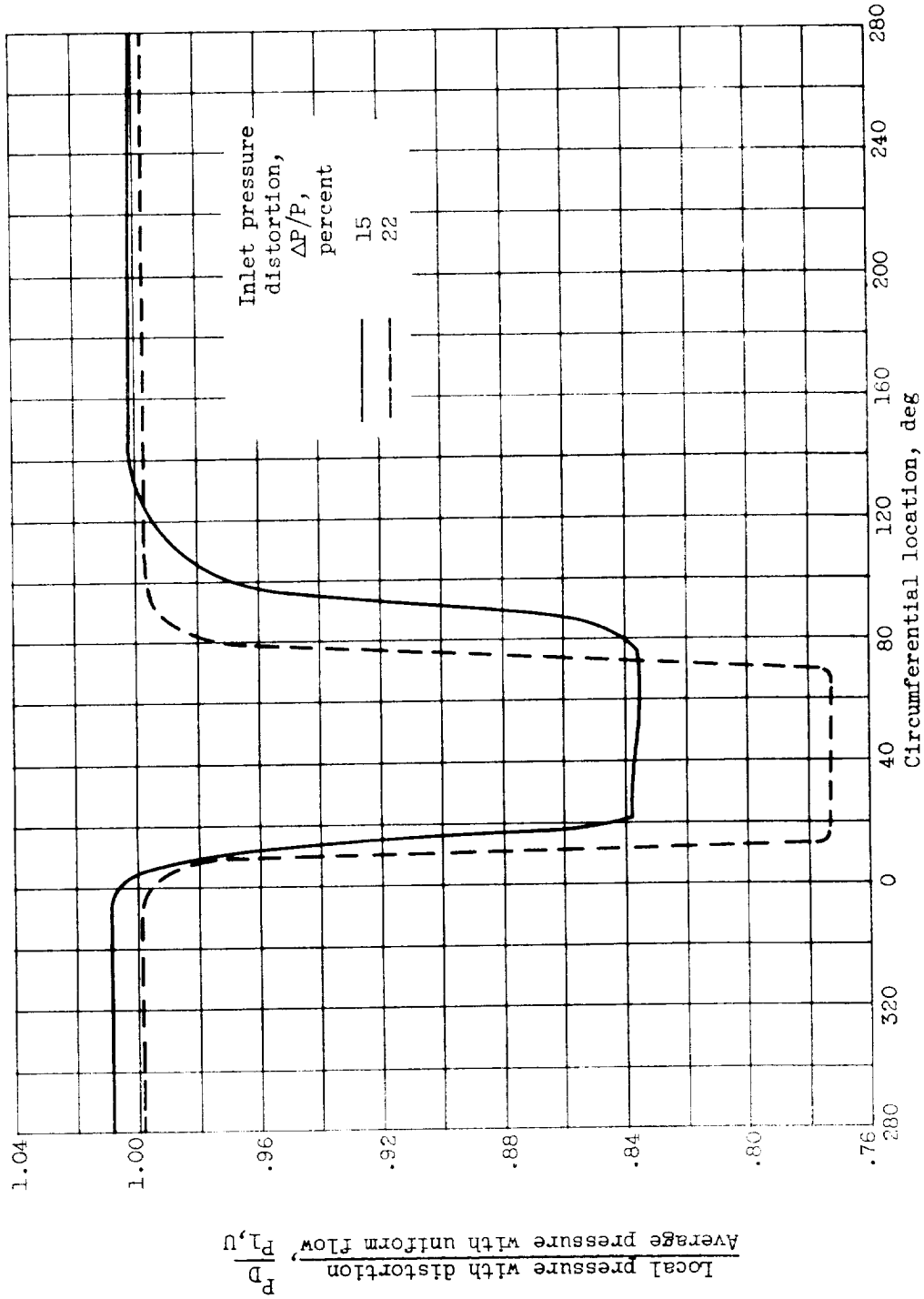


(a) Sector angle, 70°.

Figure 5. - Total-pressure profiles at inlet guide vanes (midspan). Corrected engine speed, 7800 rpm.

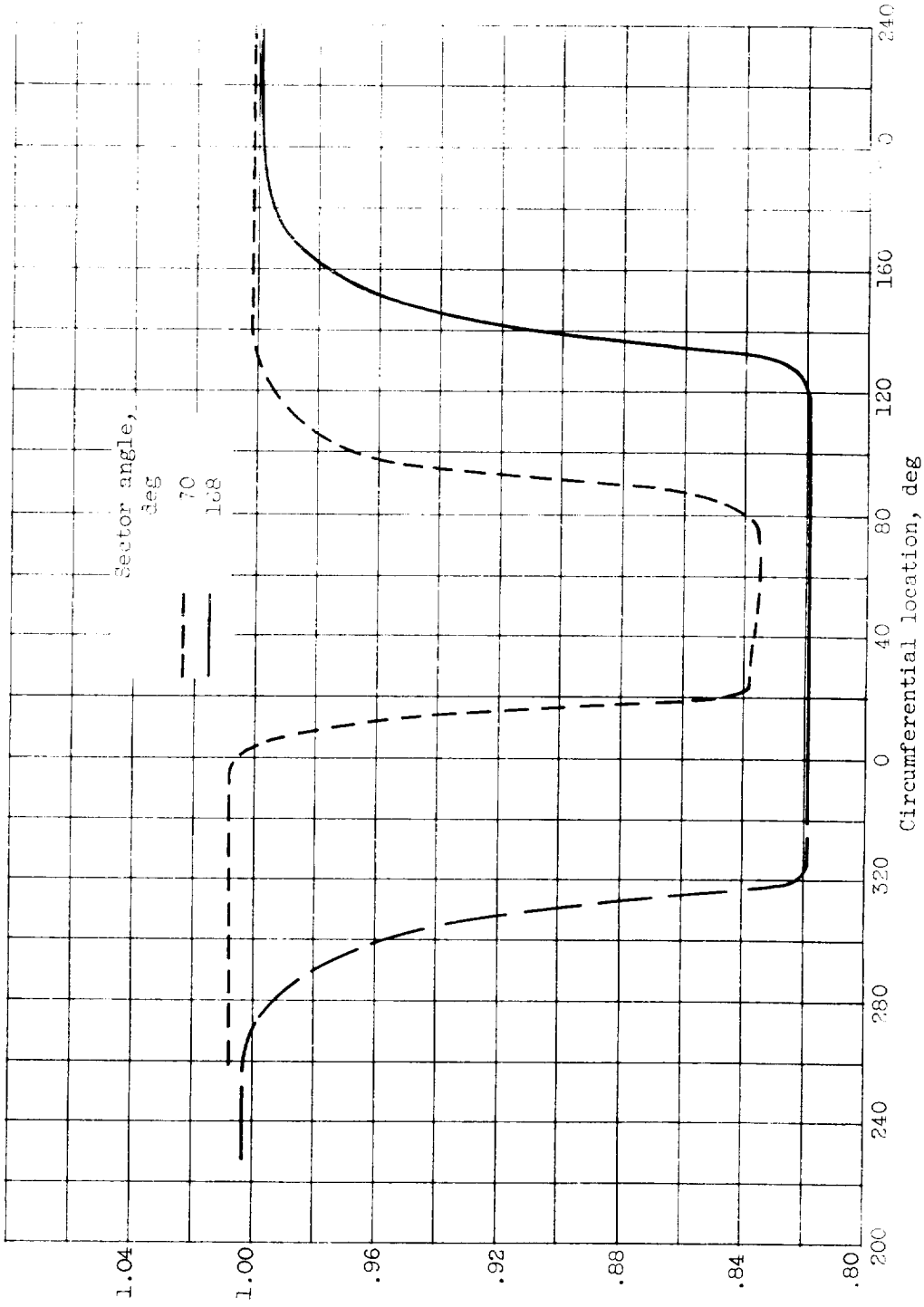


(b) Inlet pressure distortion, 15 percent.

Figure 5. - Concluded. Total-pressure profiles at inlet guide vanes (midspan). [illegible] ted engine speed, 7800 rpm.

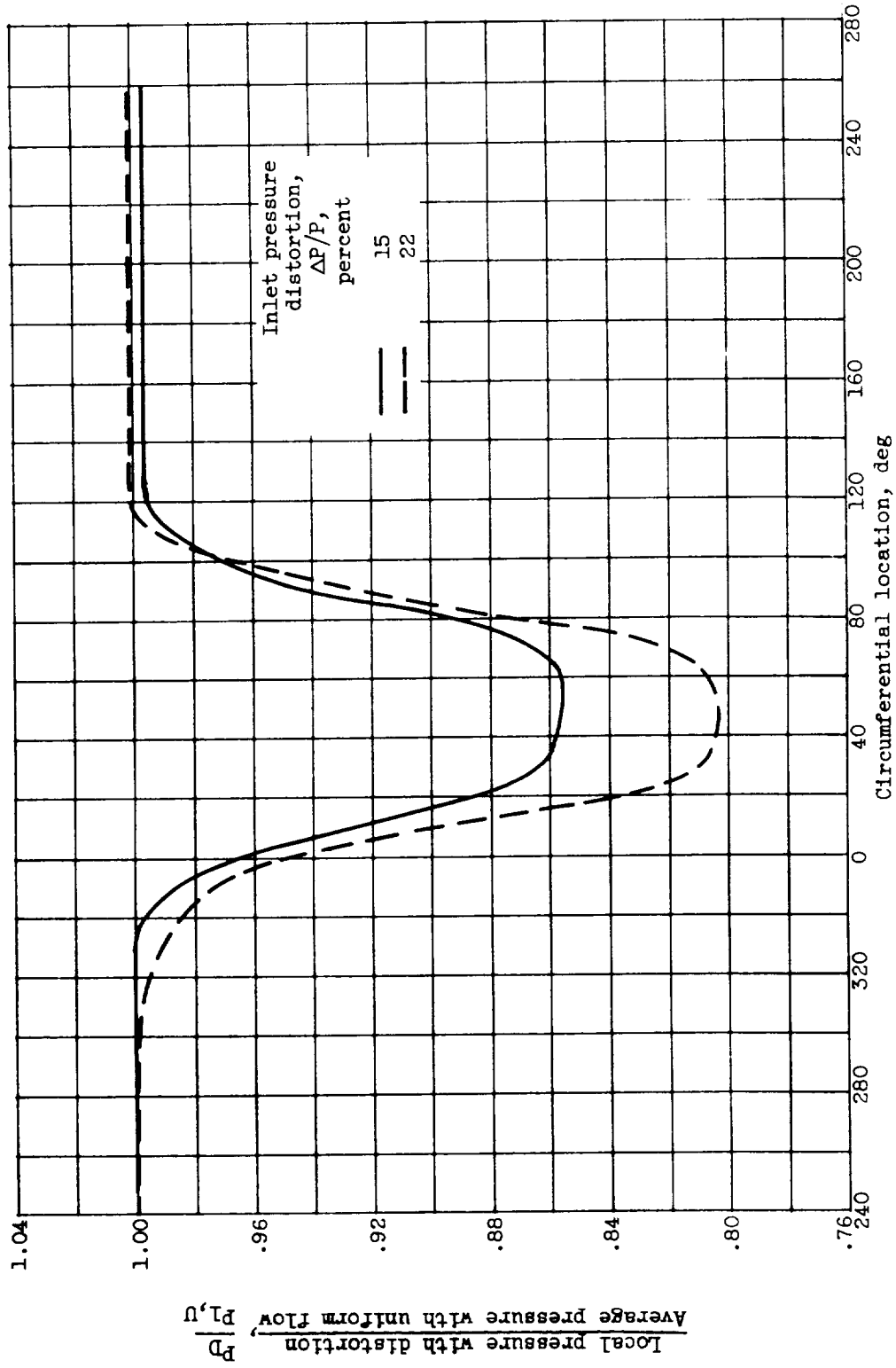


(a) Sector angle, 70°.

Figure 6. - Static-pressure profiles taken 4 inches upstream of inlet guide vanes (midspan). Corrected engine speed, 7800 rpm.

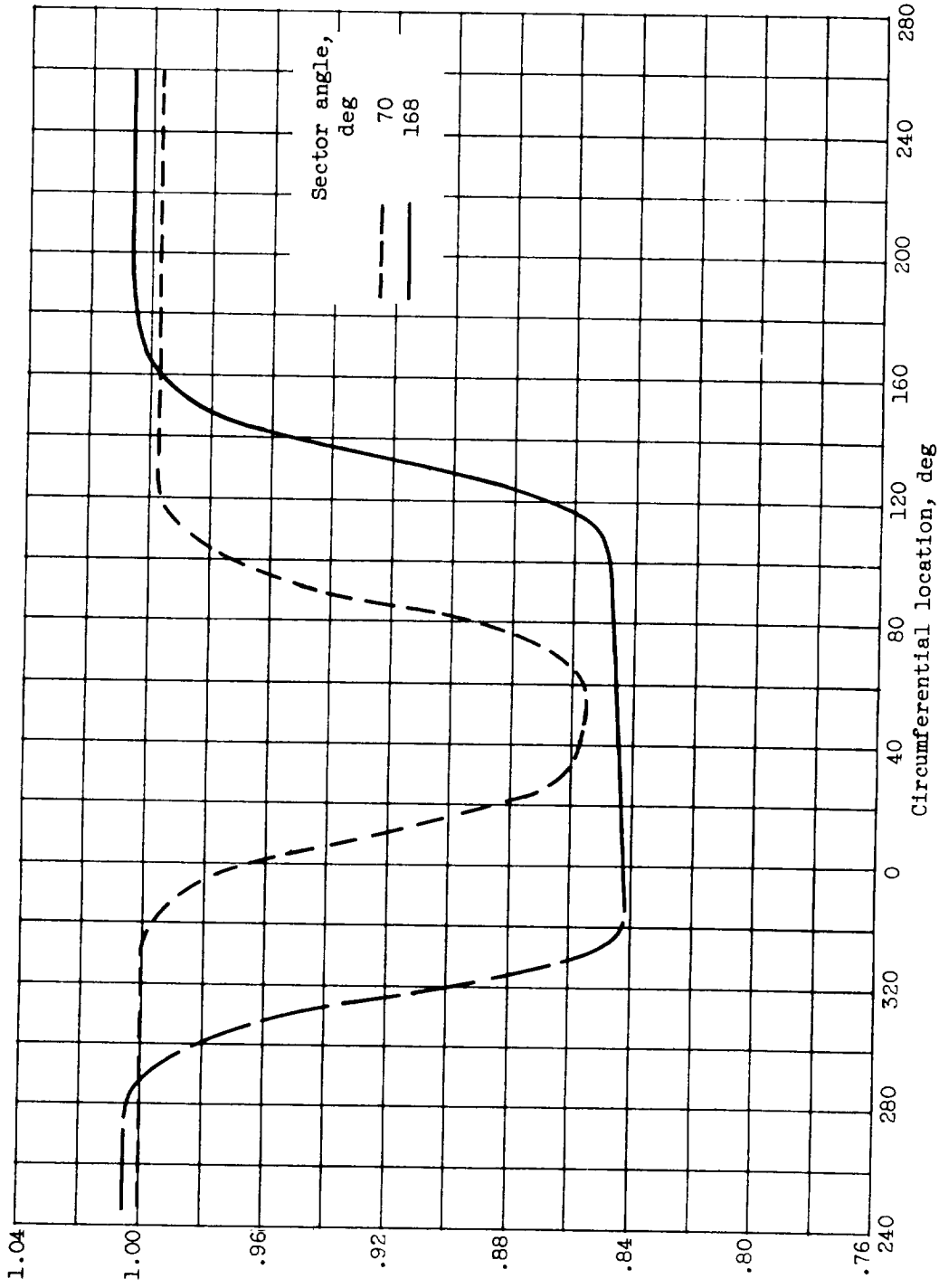


(b) Inlet pressure distortion, 15 percent

Figure 6. - Concluded. Static-pressure profiles taken 4 inches upstream of inlet guide vanes (midspan). Corrected engine speed, 7800 rpm.

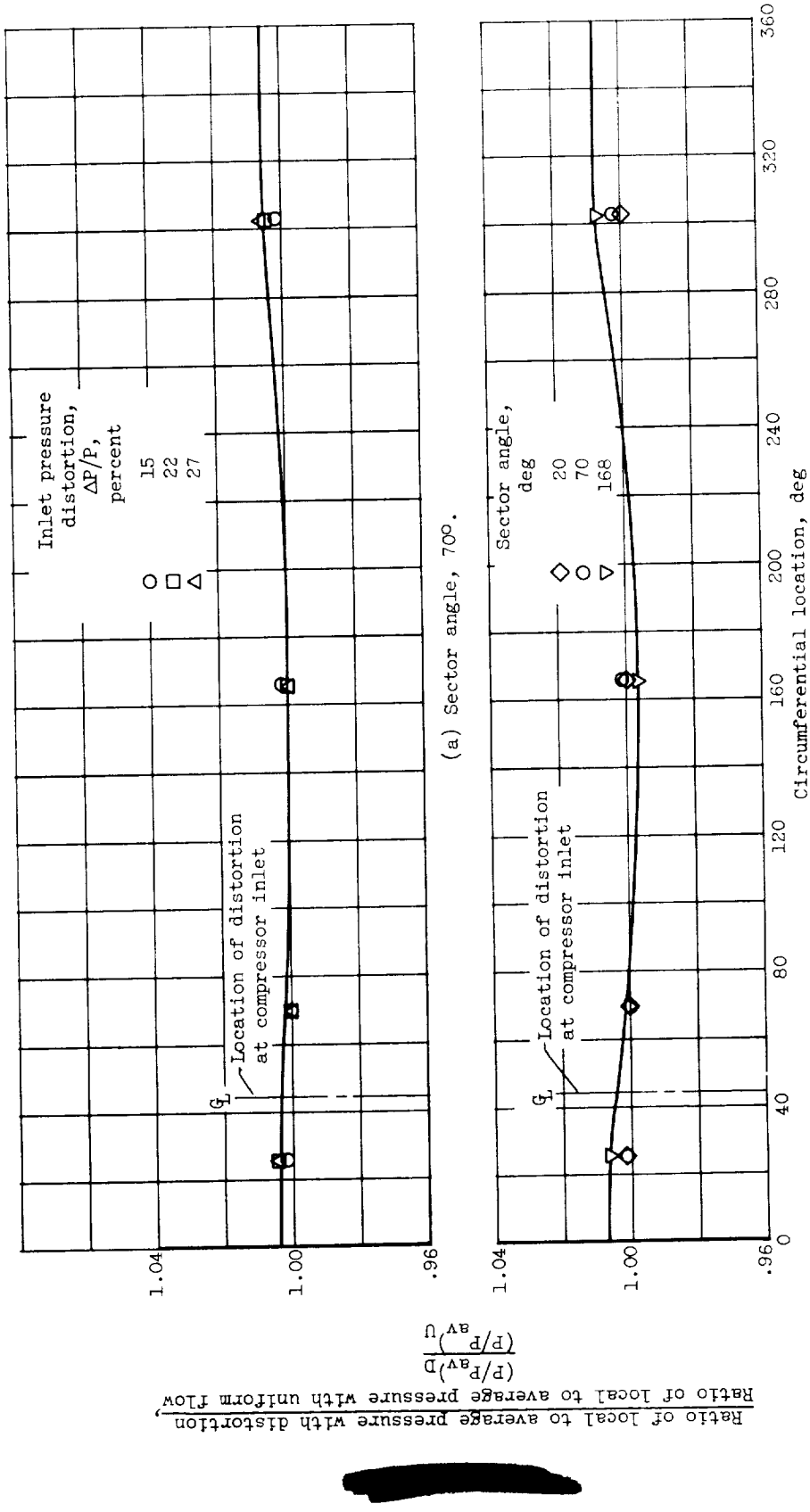


Figure 7. - Total-pressure profiles at compressor outlet (midpassage). Corrected engine speed, 7800 rpm.

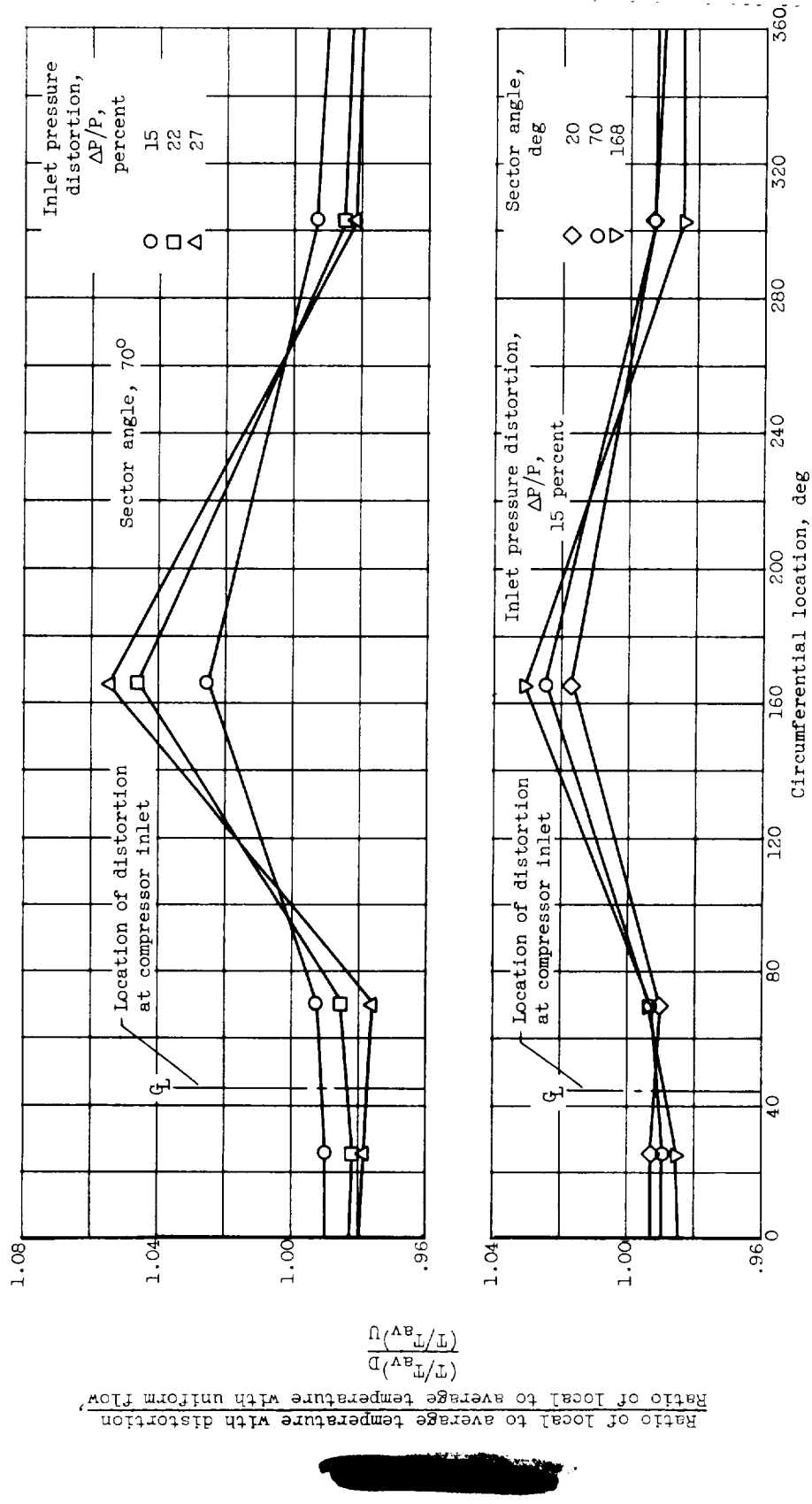


(a) At compressor outlet.

Figure 8. - Midspan total-temperature profiles. Corrected engine speed, 7800 rpm.

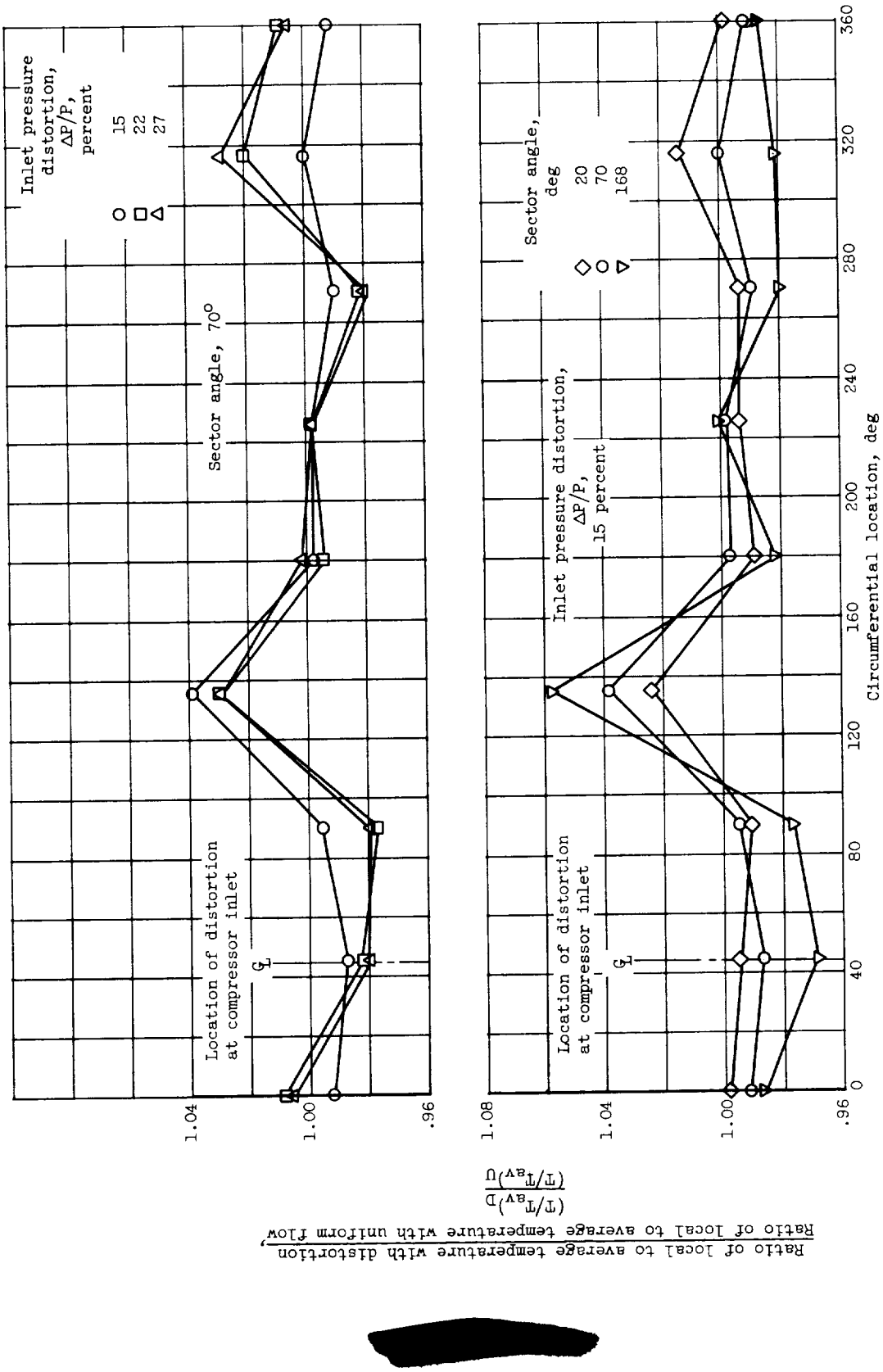


(b) At turbine outlet.

Figure 8. - Concluded. Midspan total-temperature profiles. Corrected engine speed, 7800 rpm.

4634

CI-4 back

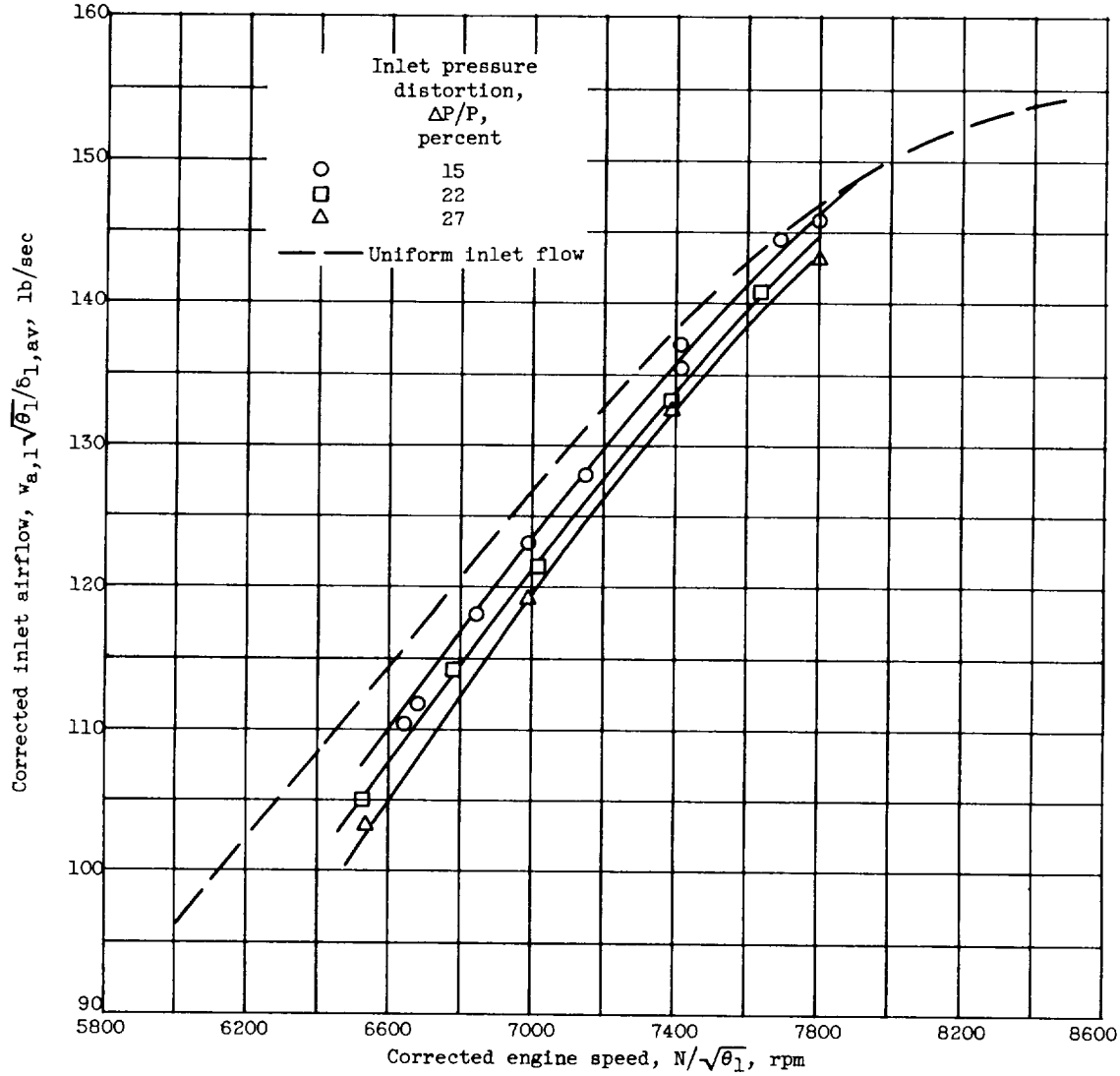


(a) Corrected inlet airflow. Sector angle, 70°.

Figure 9. - Effect of inlet pressure distortion and sector angle on compressor performance.

[redacted]

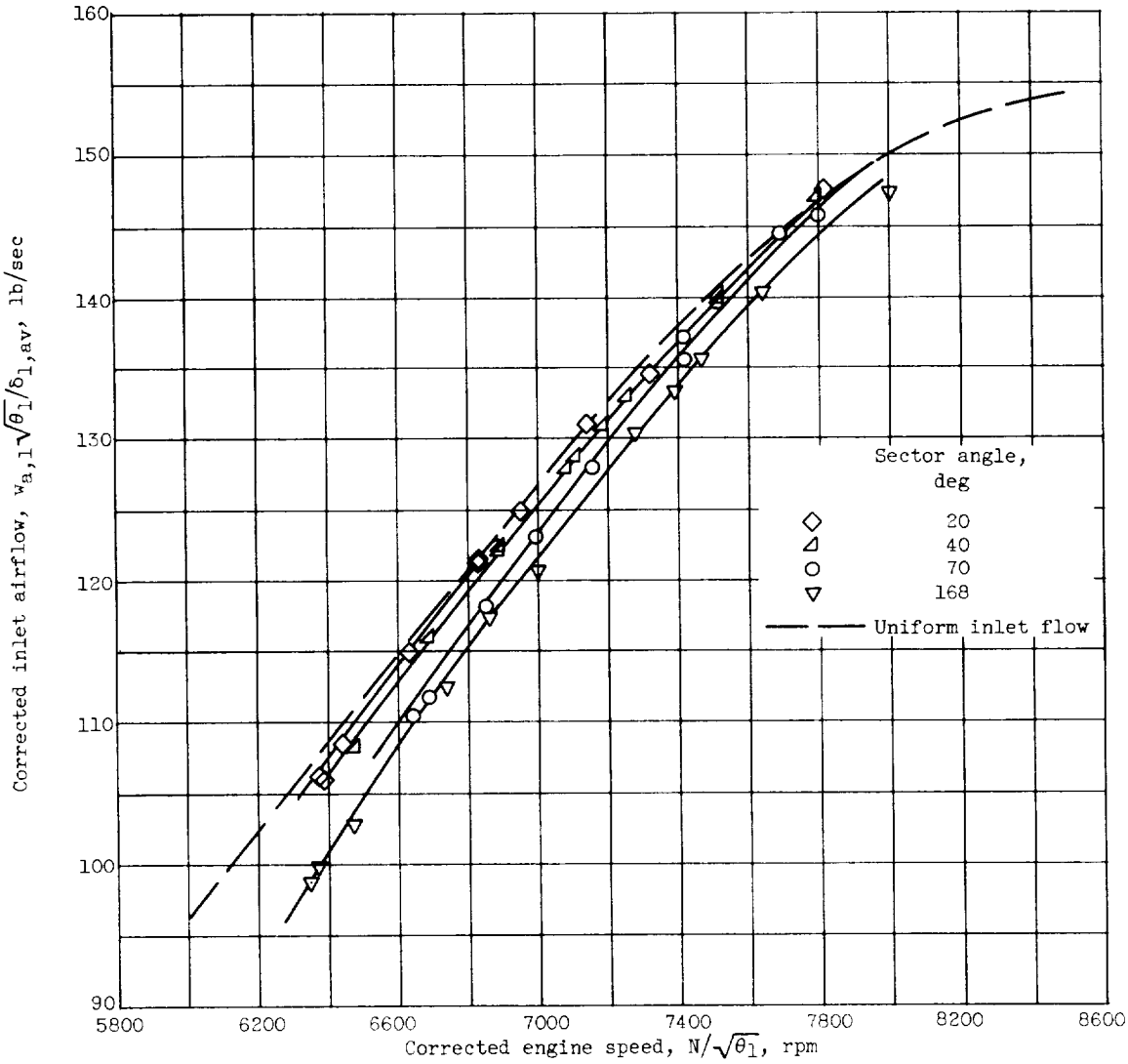


(b) Corrected inlet airflow. Inlet pressure distortion, 15 percent.

Figure 9. - Continued. Effect of inlet pressure distortion and sector angle on compressor performance.

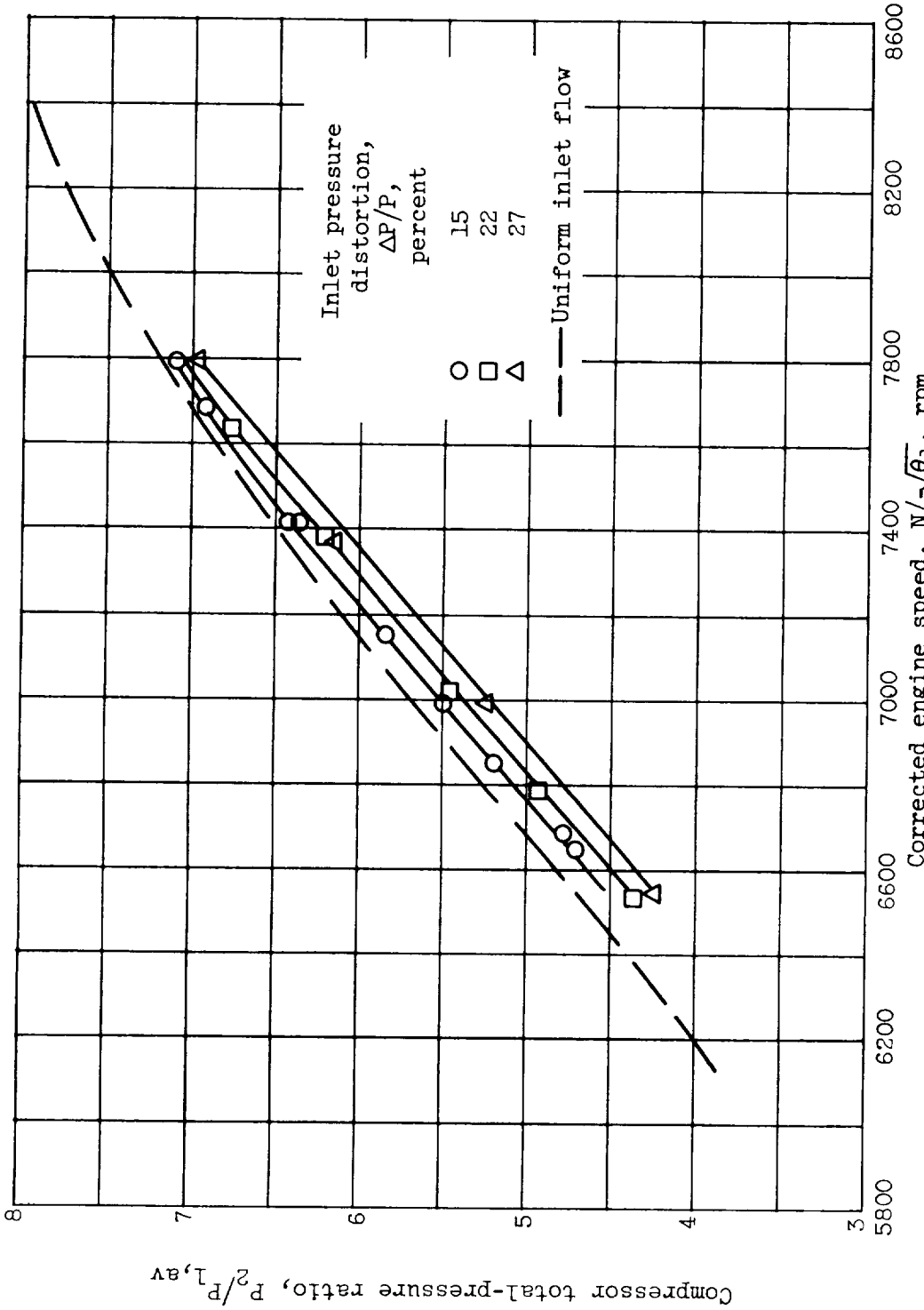


(c) Pressure ratio. Sector angle, 70°.

Figure 9. - Continued. Effect of inlet pressure distortion and sector angle on compressor performance.

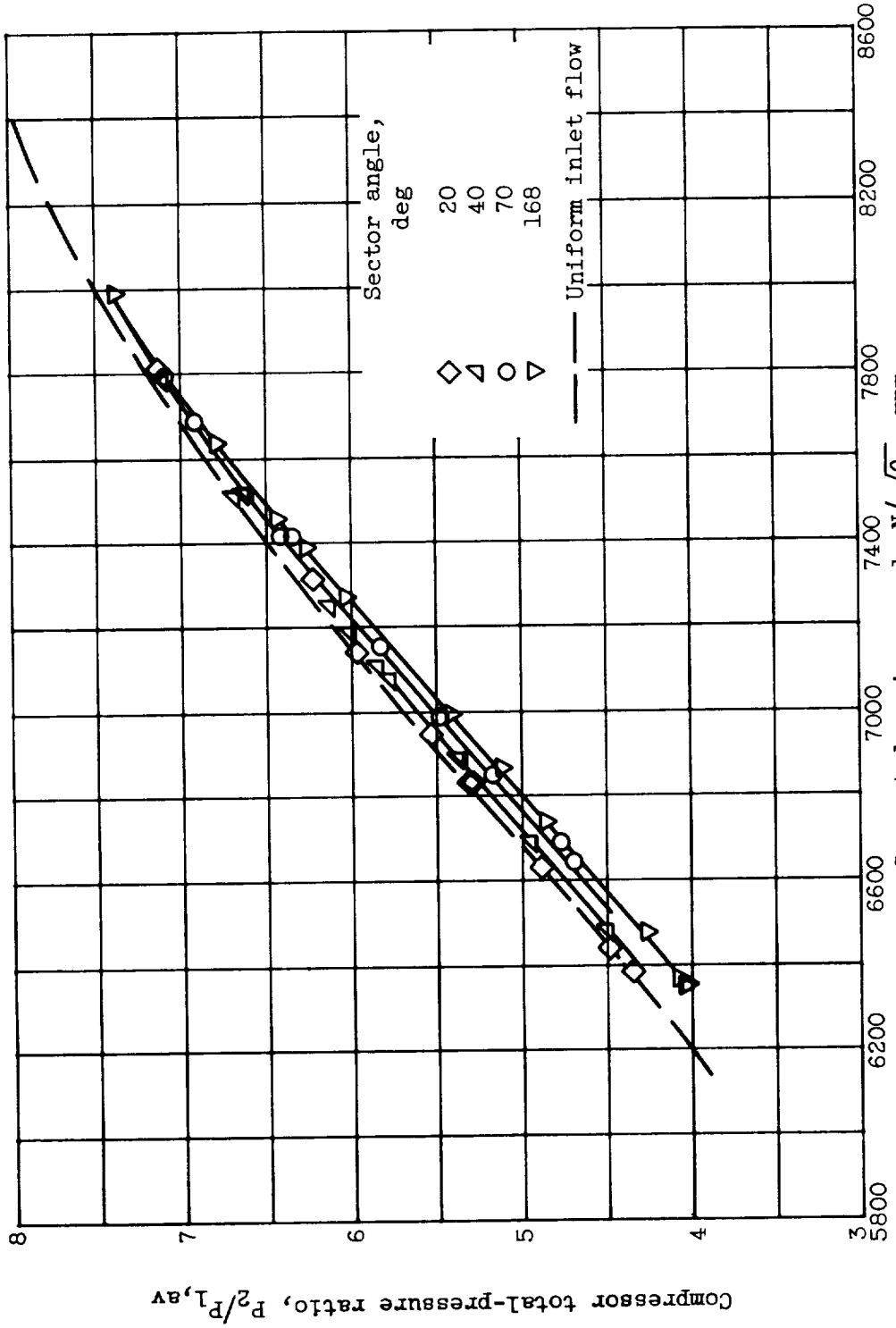


(d) Pressure ratio. Inlet pressure distortion, 15 percent.

Figure 9. - Continued. Effect of inlet pressure distortion and sector angle on compressor performance.

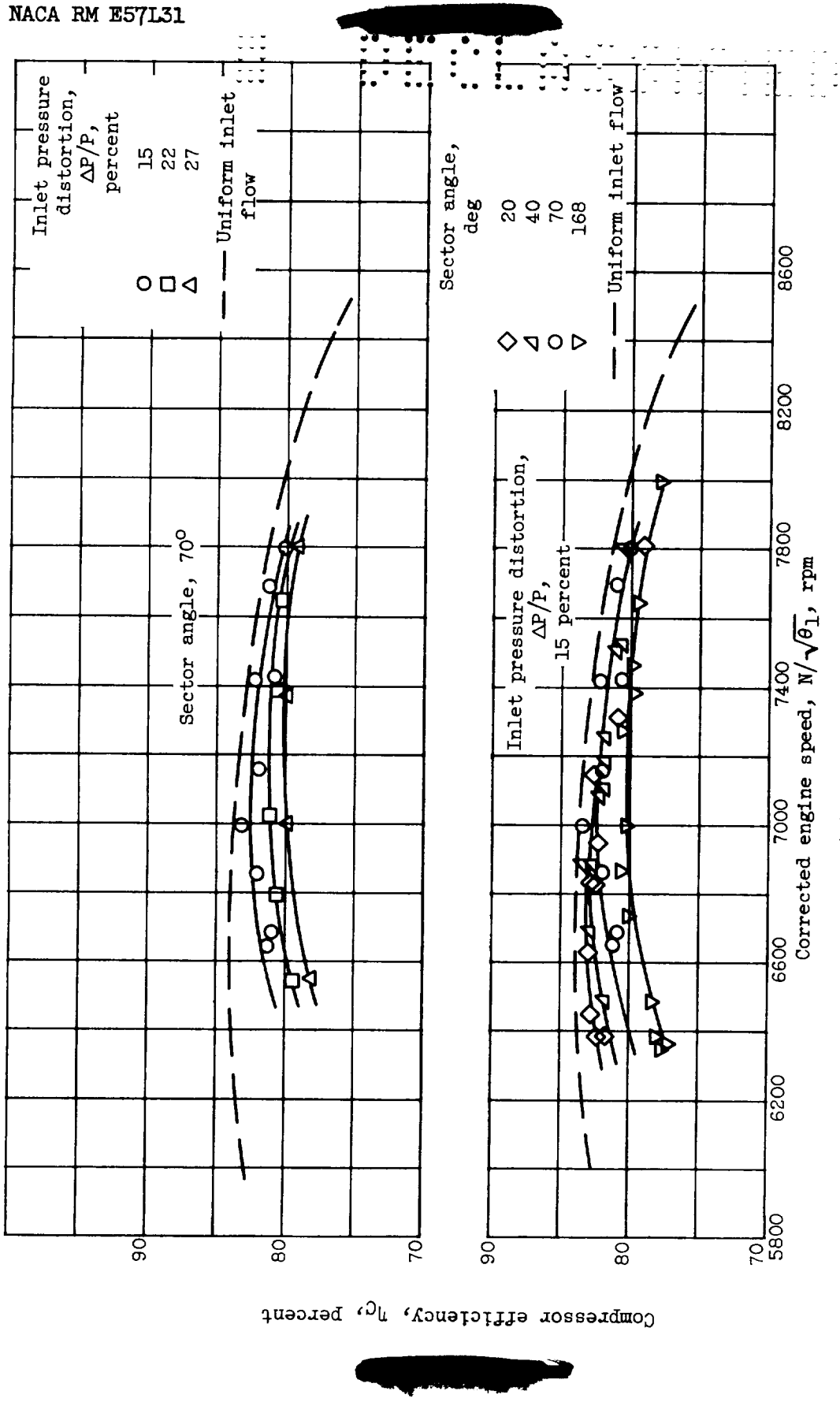


(e) Efficiency.

Figure 9. - Concluded. Effect of inlet pressure distortion and sector angle on compressor performance.

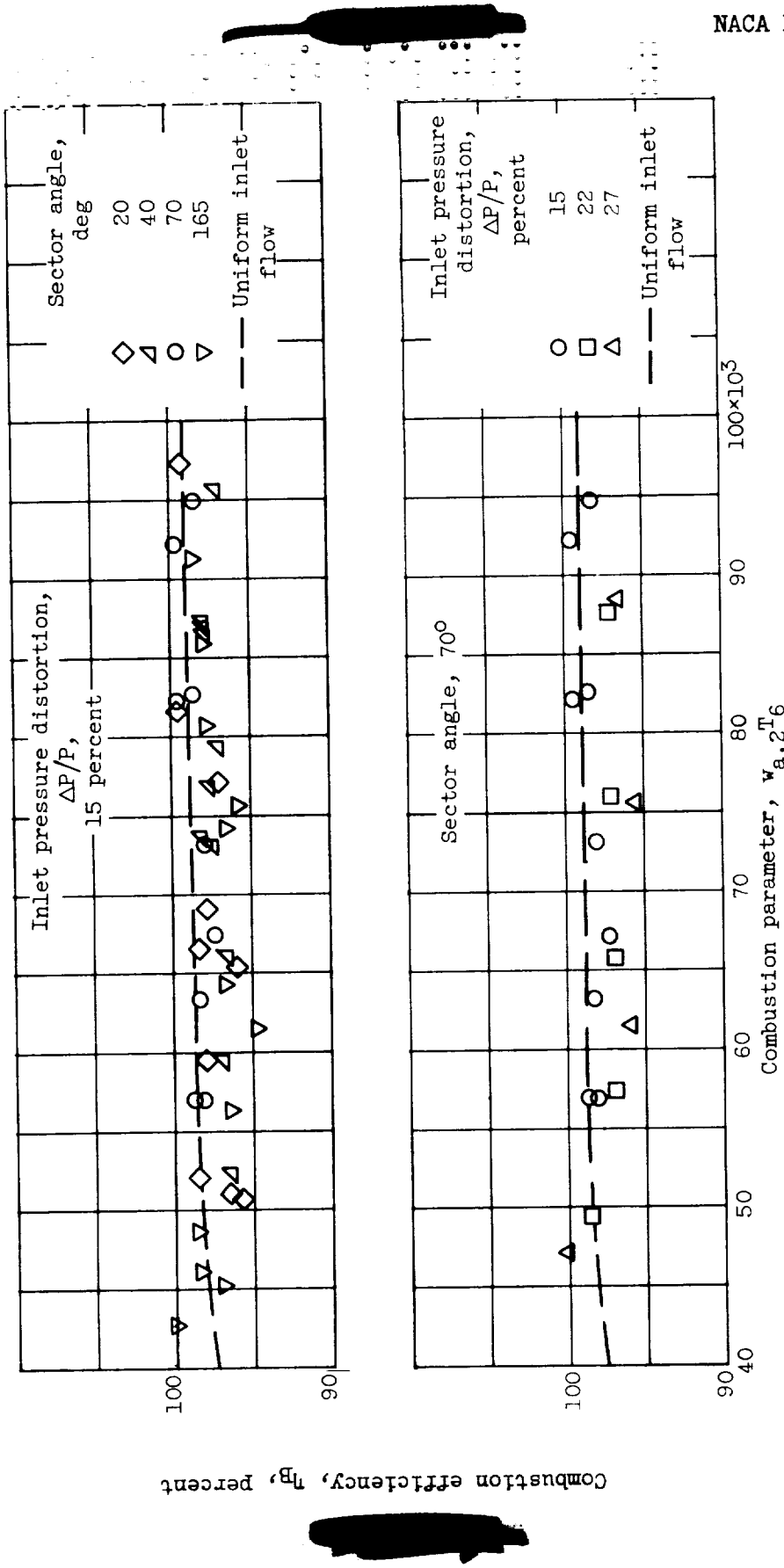


Figure 10. - Effect of inlet pressure distortion and sector angle on combustion efficiency.

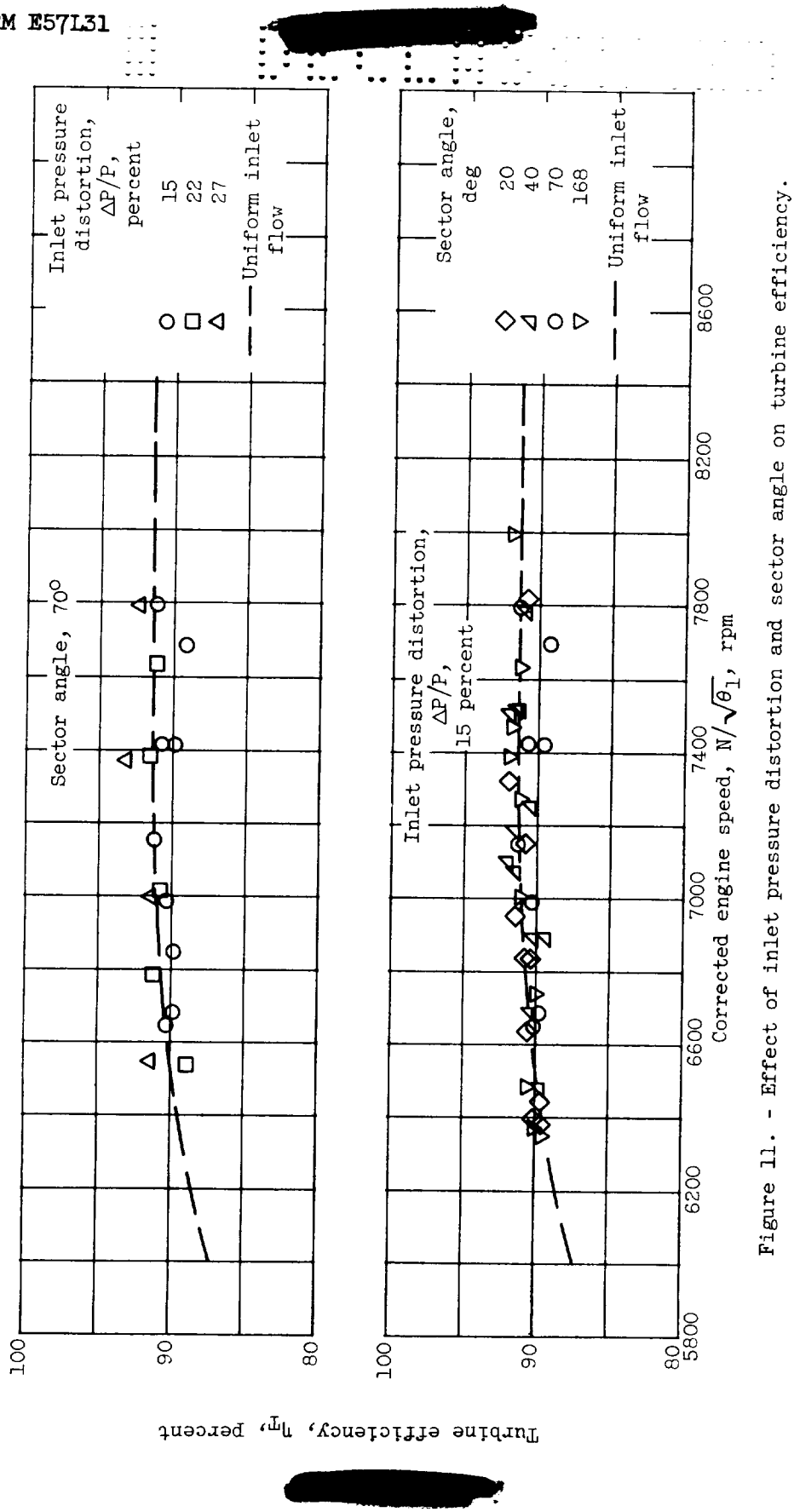


Figure 11. - Effect of inlet pressure distortion and sector angle on turbine efficiency.

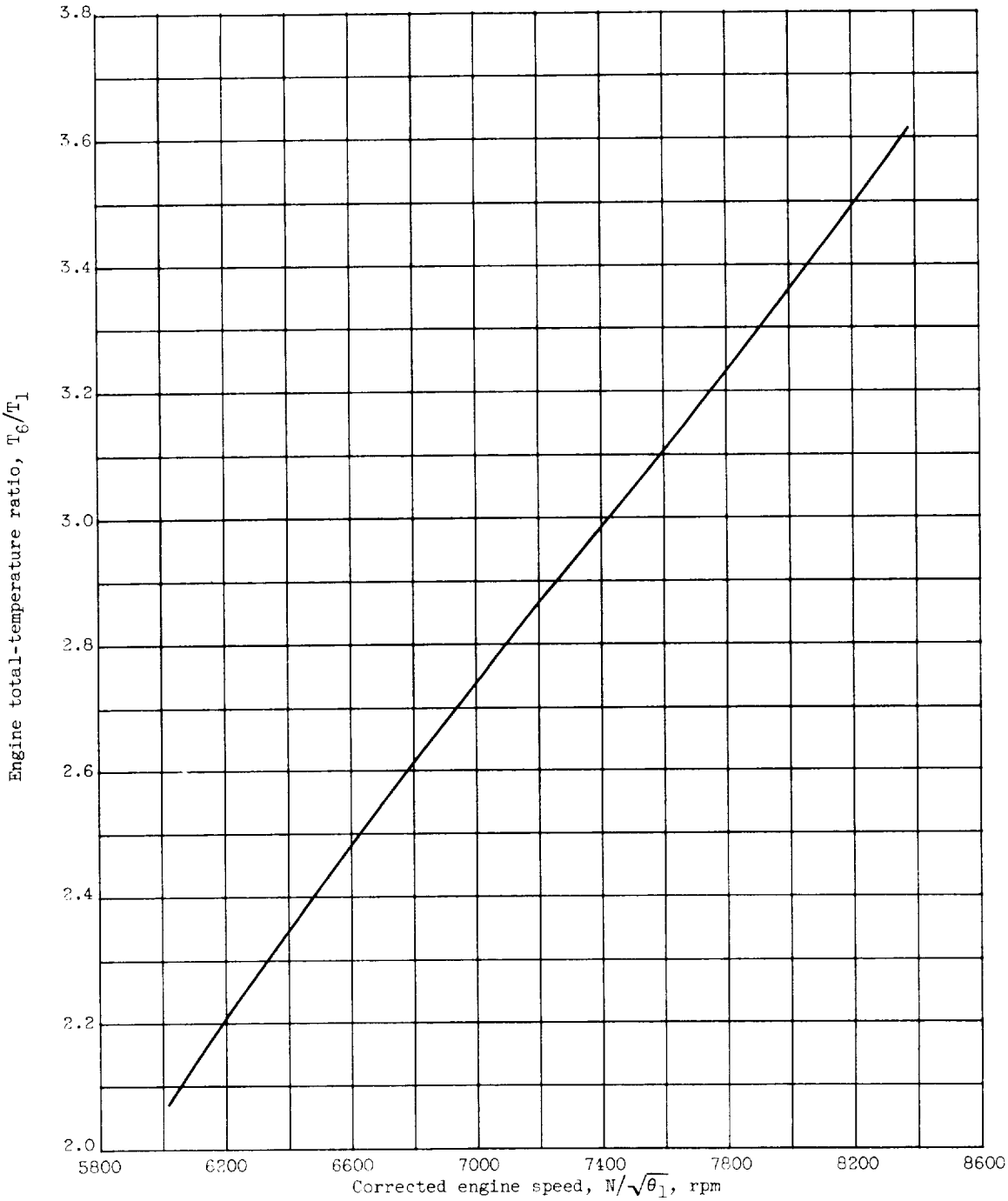


Figure 12. - Engine total-temperature ratio as function of corrected engine speed.

[redacted]

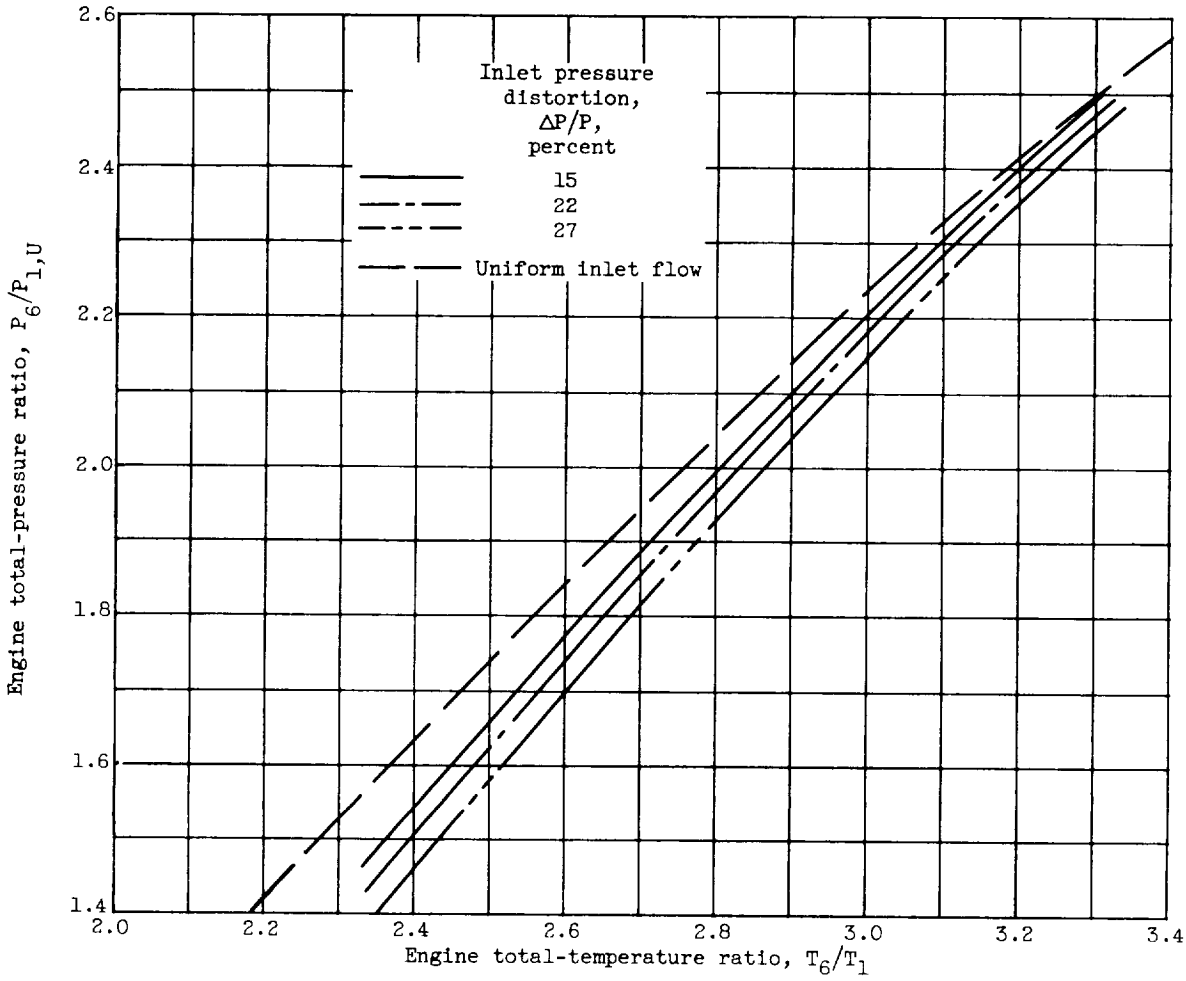


(a) Sector angle, 70°.

Figure 13. - Effect of inlet pressure distortion and sector angle on engine pumping characteristics.

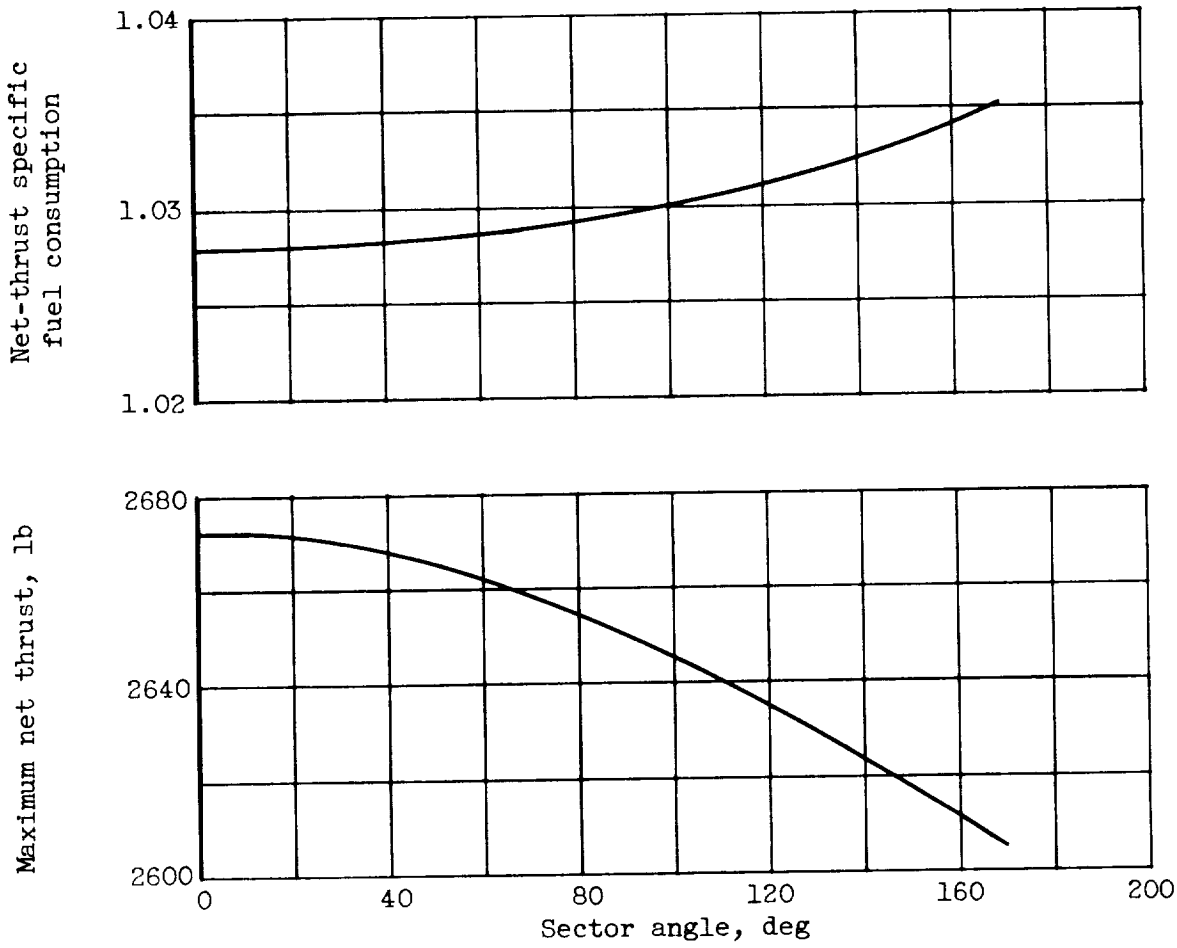


(b) Sector angle.

Figure 14. - Concluded. Effect of inlet pressure distortion and sector angle on maximum net thrust and net-thrust specific fuel consumption. Altitude, 35,000 feet; flight Mach number, 0.8; rated corrected engine speed and exhaust-nozzle area.

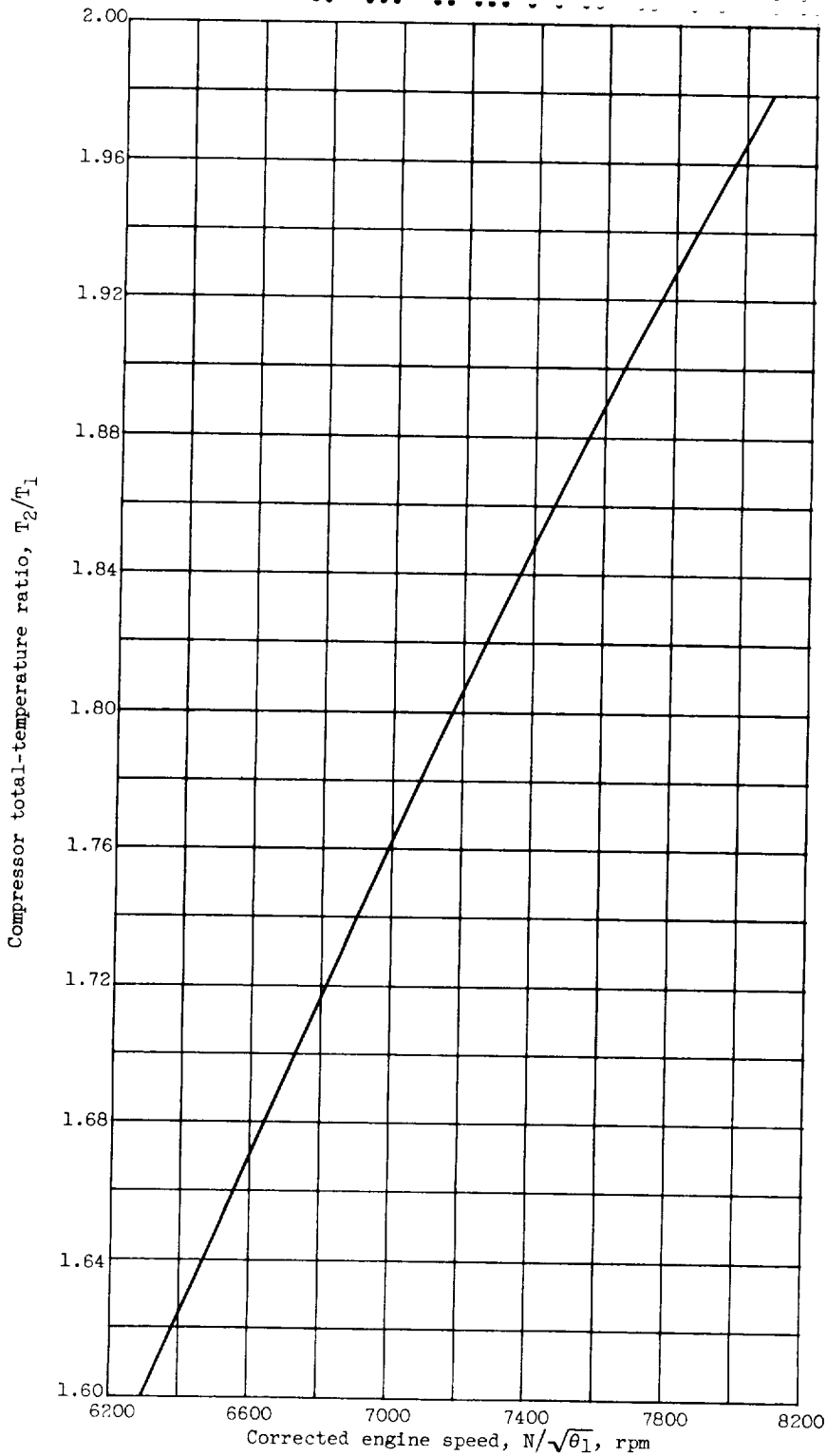


Figure 15. - Compressor total-temperature ratio as function of corrected engine speed.

[redacted]

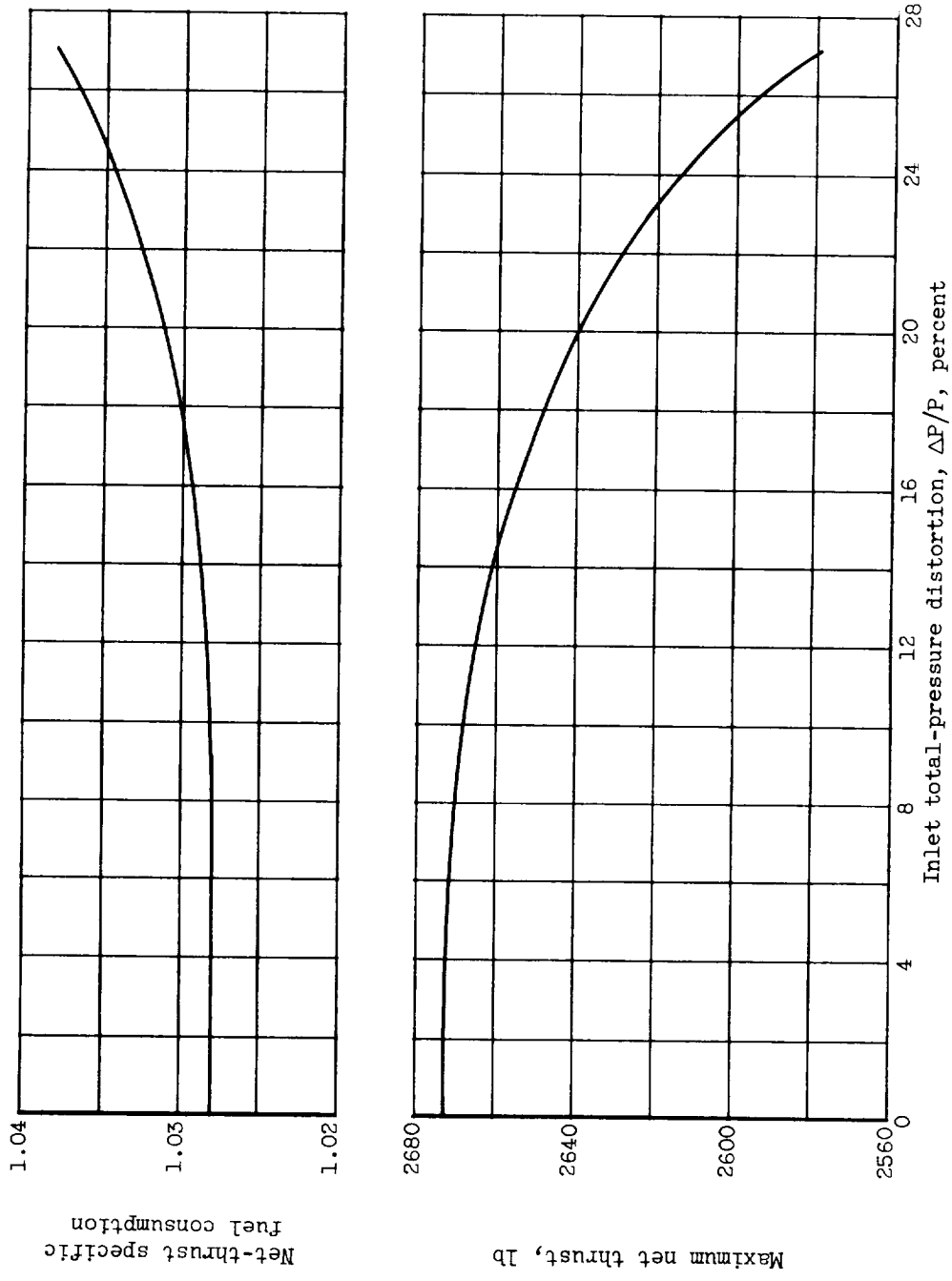


(a) Inlet pressure distortion.

Figure 14. - Effect of inlet pressure distortion and sector angle on maximum net thrust and net-thrust specific fuel consumption. Altitude, 35,000 feet; flight Mach number, 0.8; rated corrected engine speed and exhaust-nozzle area.

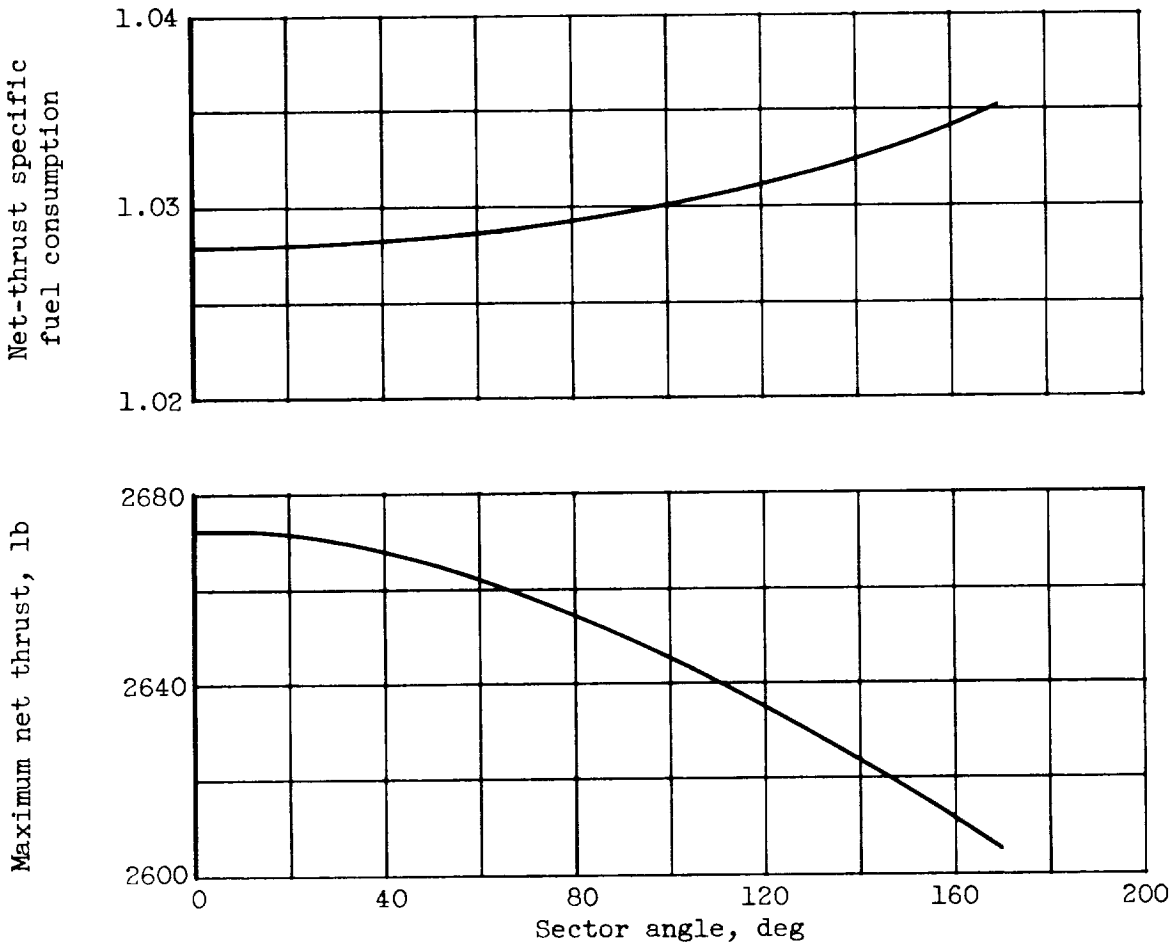


(b) Sector angle.

Figure 14. - Concluded. Effect of inlet pressure distortion and sector angle on maximum net thrust and net-thrust specific fuel consumption. Altitude, 35,000 feet; flight Mach number, 0.8; rated corrected engine speed and exhaust-nozzle area.

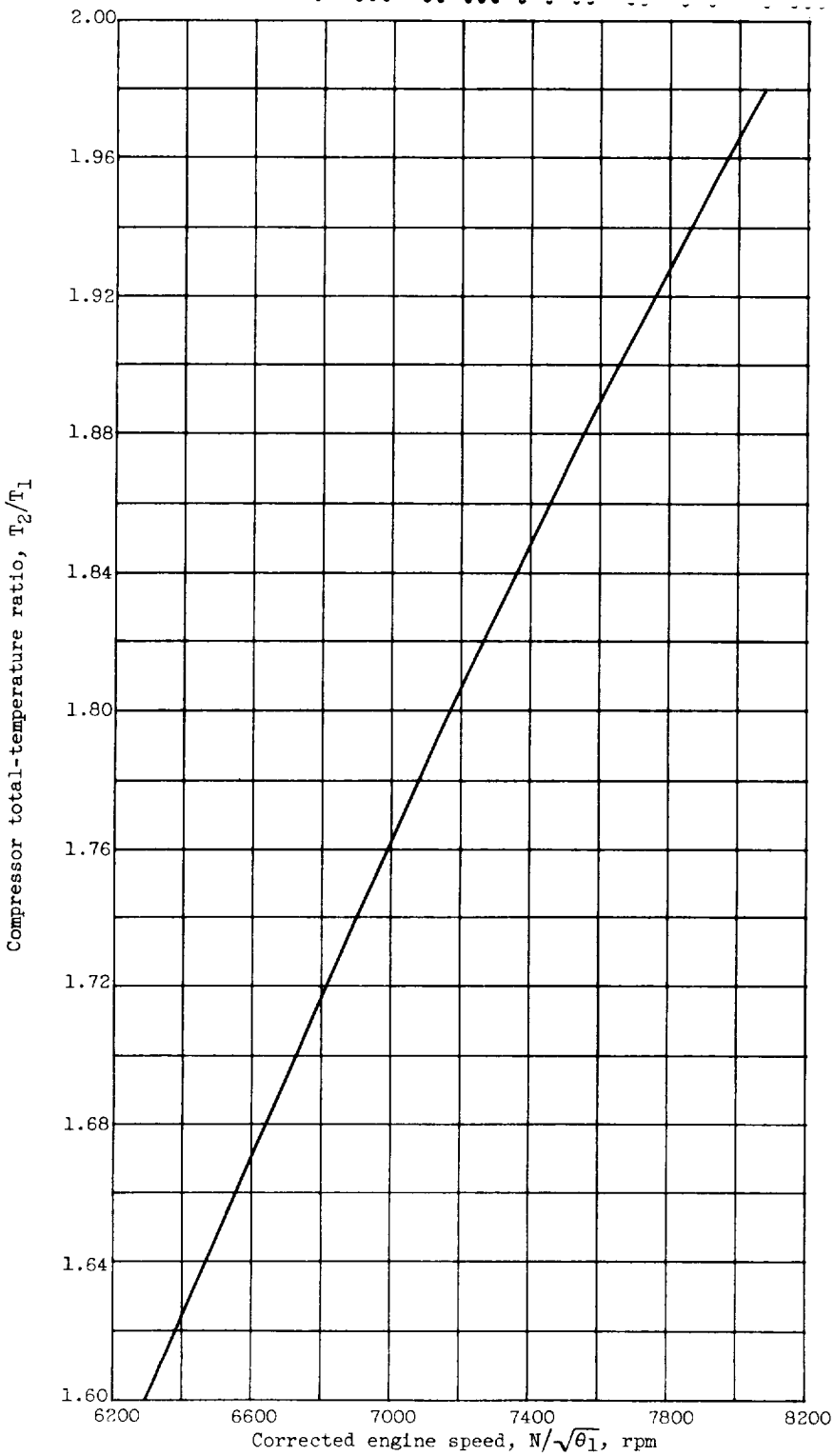


Figure 15. - Compressor total-temperature ratio as function of corrected engine speed.

NACA RM E57L31 [redacted]

# EFFECTS OF INLET AIR DISTORTION ON STEADY-STATE PERFORMANCE OF AN AXIAL-FLOW TURBOJET ENGINE

4634


Robert E. Russey

Ferris L. Seashore


Approved:

E. William Conrad
Chief
Engines Branch

Bruce T. Lundin
Chief
Propulsion Systems Division

maa - 1/3/58

[redacted]

NACA-CLEVELAND